UNIVERSITA' POLITECNICA DELLE MARCHE

FACOLTA' DI **INGEGNERIA**

Corso di Laurea magistrale **GREEN INDUSTRIAL ENGINEERING**

Performance analysis of a hydrogen production plant: Efficiency evaluation of a NaOH alkaline electrolyzer

Relatore: Chiar.mo

Prof. Ing. **Gabriele Comodi**

Correlatore:

Dott. Ing. **Mosè Rossi**

Tesi di Laurea di:

Enrik Xhani

A.A. **2023 /2024**

Content

ABBREVIATIONS

EPT	- Energy Payback Time
PV	- Photovoltaic
EROEI	- Energy Return on Energy Invested
IRMs	- Inorganic mineral Raw Materials
EU	- European Union
GHG	- Green House Gases
TES	- Total Energy Supply
IEA	- International Energy Agency
LDVs	- Light-Duty Vehicles
CAPEX	- Capital Expenditure
OPEX	- Operational Expenditure
ECH_2A	- European Clean Hydrogen Alliance
CHP	- Combined Heat and Power
Mtoe	- Million Tonnes of Oil Equivalent
SMR	- Steam Methane Reforming
PEM	- Proton Exchange Membrane
AWE	- Alkaline Water Electrolysis
AEM	- Anion Exchange Membrane
SOE	- Solid Oxide Electrolysis
SOECs	- Solid Oxide Electrolysis Cells
P2G2P	- Power-to-Gas-to-Power
DIISM	- Department of Industrial Engineering and Mathematical Sciences
HE	- Heat Exchanger
RE	- Renewable Energy
NECP	- National Energy and Climate Plan
NRRP	- National Recovery and Resilience Plan
RES	- Renewable Energy Sources
CCS	- Carbon Capture and Storage
RED	- Renewable Energy Directive
ICE	- Internal Combustion Engines
LH_2	- Liquid Hydrogen
MiTE	- Ministry for the Ecological Transition
FEC	- Final Energy Consumption
LTS	- Long-Term Strategy
R&D	- Research and Development
FF55	- Fit-For-55
MEAs	- Membrane Electrode Assemblies
Pt/Pd	- Platinum/Palladium
IrO_2/RuO_2	- Iridium dioxide/Ruthenium dioxide
PHEV	- Plug-in Hybrid Electric Vehicle
MoS_2	- Molybdenum Disulfide
BEV	- Battery Electric Vehicle
LNG	- Liquefied Natural Gas
LPG	- Liquefied Petroleum Gas
CNG	- Compressed Natural Gas

INTRODUCTION

The provision of clean, efficient, affordable, and reliable energy services is essential for fostering global prosperity and achieving sustainable development goals. The world's total energy supply has undergone significant changes over the years, reflecting shifts in energy demand, technological advancements, policy interventions, and evolving market dynamics. Concerns about environmental pollution, energy security, and climate change increased interest in renewable energy sources such as hydropower, wind, solar, and biomass.

The aim is to achieve two primary goals: ensuring universal energy access and reducing global energy intensity. These actions are directed towards various stakeholders, including governments, multilateral institutions, private sectors, and non-profit organizations.

One central goal of the Paris Agreement is keeping global warming below 1.5°C to ensure a climate-resilient world. Despite progress, current efforts fall short of closing the emissions gap, emphasizing the urgent need for ambitious action and robust progress in building resilience.

The scope of this thesis encompasses a comprehensive analysis of the current state of energy sustainability, focusing on renewable energy adoption and its implications. It entails examining the feasibility, effectiveness, and potential challenges associated with integrating hydrogen renewable into existing energy systems.

Opportunities exist to accelerate climate action across various systems and sectors, but they need to be scaled up. Identifying and addressing challenges and barriers to deployment is crucial to increasing climate actions' pace and scale.

The topic of this thesis aligns with **SDG 7 (Ensure access to affordable, reliable, sustainable, and modern energy for all)** which envisions a fundamental transformation of the global energy system by 2030, with countries shifting to cleaner, sustainable, and reliable energy services. Achieving this transformation requires substantial regulatory reforms, infrastructure investments, accelerated development and deployment of new technologies, and a shift in energy consumption behaviour.

While uneven progress and potential energy security crises are risks, effective energy system transformation can lead to sustainable wealth creation and alleviate resource and climate strain. Energy access and energy efficiency are presently identified as immediate actionable areas with numerous co-benefits, highlighting their critical role in achieving broader energy system goals.

A significant component of the thesis involves the performance evaluation of an alkaline electrolyser, a central component to foster the production of green hydrogen. This entails detailing the technological specifications, operational processes, and potential benefits of utilizing green hydrogen as a clean and renewable energy source. The analysis will explore the feasibility and scalability of green hydrogen production and utilization, highlighting its role in decarbonizing energy systems and achieving climate mitigation objectives.

By addressing these objectives and putting an emphasis on green hydrogen production, the thesis aims to contribute valuable insights to the discourse on energy sustainability and provide actionable recommendations to accelerate the transition towards a cleaner, more sustainable energy future.

CHAPTER 1 - BUILDING A SUSTAINABLE FUTURE: CHALLENGES AND OPPORTUNITIES

We encounter challenges and opportunities in our journey towards a sustainable future. As we tackle issues like pollution, resource depletion, and climate change, the need to create a sustainable world becomes more urgent. Striving to meet the world's growing energy demands while reducing environmental impact requires a thorough understanding of the complexities of sustainability within the energy sector, exploring how we can harness renewable resources, optimize energy production and consumption, and mitigate climate change. By examining the intersection of energy production, distribution, and consumption with sustainability principles, we can uncover innovative solutions that pave the way toward a cleaner, more resilient energy future.

1.1 Energy Needs: Global Perspectives

Energy lies at the core of numerous critical global challenges spanning economic, environmental, and social spheres. The provision of clean, efficient, affordable, and reliable energy services is essential for fostering global prosperity and achieving sustainable development goals. Particularly in developing countries, expanding access to modern energy services is imperative for poverty reduction, improved health outcomes, increased productivity, enhanced competitiveness, and overall economic growth.

A well-functioning energy system that facilitates efficient access to modern

energy forms holds the potential to uplift billions from poverty and supports broader development objectives. Economic growth is closely linked to increased access to modern energy services with underperforming energy systems potentially costing countries significant growth potential annually. Moreover, the global energy system significantly contributes to climate change, accounting for around 75% of total current greenhouse gas emissions.[1]

Unsustainable patterns of energy production and consumption exacerbate environmental degradation on both local and global scales, necessitating a shift towards reducing carbon intensity and increasing energy efficiency.

1.1.1 World's energy supply evolution

The World's Total Energy Supply has undergone significant changes over the years, reflecting shifts in energy demand, technological advancements, policy interventions, and evolving market dynamics.

Prior to the Industrial Revolution, humanity relied primarily on biomass, such as wood, for energy needs. The discovery and widespread use of coal marked the beginning of the fossil fuel era, transforming energy production and enabling industrialization.

[1] https://www.iea.org/data-and-statistics/data-tools/greenhouse-gas-emissions-from-energy-data-explorer

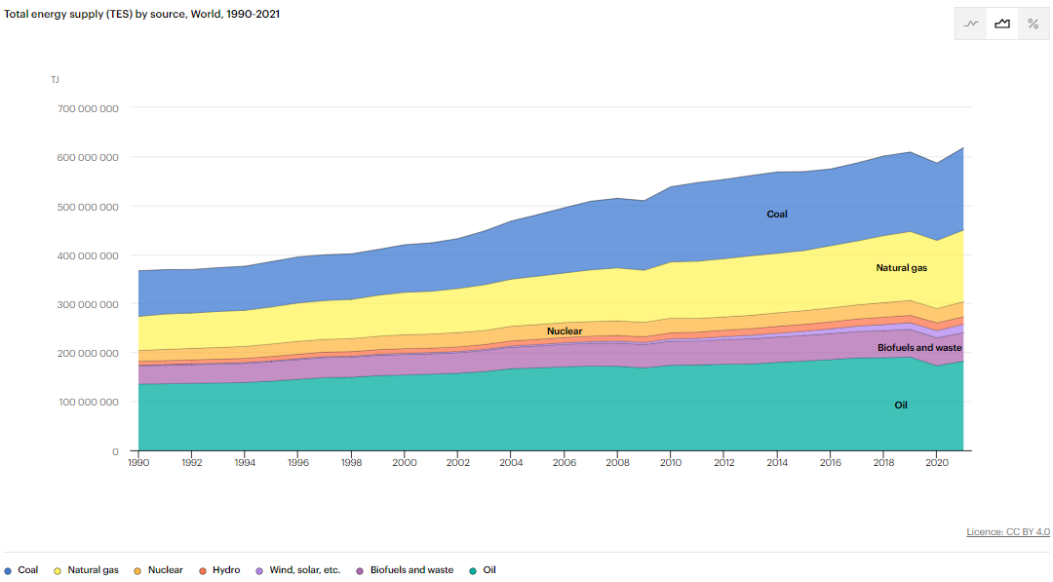

Figure 1 - Total energy supply by source, World 1990-2021 [1]

Throughout the 19th and early 20th centuries, coal was the dominant energy source, powering steam engines, factories, and transportation systems. In the early to mid-20th century, the discovery and exploitation of oil and natural gas further expanded the use of fossil fuels, particularly in transportation and electricity generation.

The mid-20th century witnessed a rapid expansion of petroleum (oil) usage, driven by the rise of the automotive industry and increased demand for gasoline and diesel fuels. Natural gas emerged as a significant energy source for heating, electricity generation, and industrial processes supported by advancements in extraction and distribution technologies.

Fossil fuels including coal, oil, and natural gas continued to dominate the global energy mix into the late 20th century, accounting for most of the total energy supply.

Concerns about environmental pollution, energy security, and climate change increased interest in renewable energy sources such as hydropower, wind, solar, and biomass. The late 20th century saw the emergence of renewable energy technologies with notable growth in hydropower capacity and the development of early wind and solar technologies.

In the 21st century, advances in renewable energy technology, coupled with declining costs and supportive policies, led to a rapid expansion of renewable energy capacity worldwide. Wind and solar photovoltaic (PV) technologies experienced particularly significant growth, becoming increasingly competitive with fossil fuels in terms of cost and deployment.

The energy transition towards a more diversified and sustainable energy mix is underway, driven by efforts to reduce greenhouse gas emissions, enhance energy security, and promote sustainable development.

Governments, businesses, and communities are increasingly investing in clean energy technologies and transitioning away from fossil fuels, with a growing emphasis on energy efficiency, electrification, and decarbonization.

While fossil fuels continue to play a significant role in the global energy supply, their share is gradually declining as renewable energy sources increase and energy systems become more diversified and resilient.

Overall, the total energy supply by source has evolved from a heavy reliance on fossil fuels to a more diversified mix that includes renewable energy sources. This transition is expected to accelerate in the coming years as societies strive to

achieve their climate goals and build more sustainable and resilient energy systems.

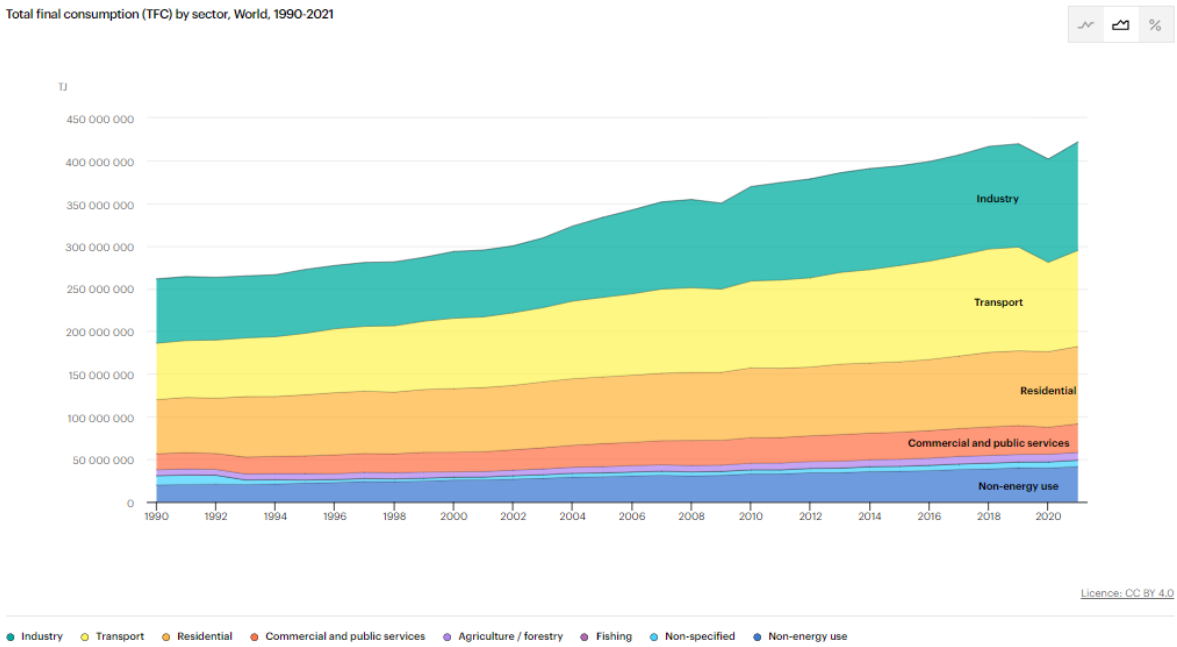

Figure 2 - Total final consumption by sector [3]

Similarly, the total energy consumption by sector has evolved in response to changing economic, social, and technological trends, with efforts increasingly focused on improving energy efficiency, reducing emissions, and transitioning to cleaner and more sustainable energy sources across all sectors.

1.2 Renewable Energy Development

Sustainable energy development on a global scale is crucial for ensuring energy security and mitigating the environmental impact of energy production and consumption. Renewable Energy (RE) emerges as a key component in this pursuit, offering alternatives to fossil fuels and addressing concerns regarding

resource availability, distribution, and variability.

Fossil fuel reserves, besides coal ones that are currently sufficient, face depletion risks in the future, particularly for oil and natural gas. Accelerated global economic growth, especially in developing regions, increases the energy demand, shortening the lifespan of these finite resources. Additionally, heavy reliance on energy imports exposes many nations to supply disruption risks and price volatility. The concentration of fossil fuel reserves in specific regions further underscores the importance of diversifying energy sources and investing in renewable alternatives that are available anywhere in the world.

Renewable energy sources offer sustainable alternatives to fossil fuels, but present challenges related to their variable availability. Solutions such as storage, technical balancing, and institutional optimizations can mitigate these challenges, but they come with additional costs that must be considered. Integration of renewable energy into existing systems is feasible at low to medium penetration levels but requires active management to address concerns about system reliability and cost-effectiveness.

Improving access to affordable and reliable energy supply can have broad social and economic effects beyond fuel price impacts. It can increase productivity and reduce the need for parallel investments in infrastructure, particularly in remote and rural areas. Decentralized RE solutions are competitive in such areas, while grid-connected supply dominates denser regions.

Sustainable development requires ensuring environmental quality and

minimizing environmental pollution. Large-scale deployment of energy technologies involves environmental trade-offs, necessitating thorough assessment of environmental impacts across the entire supply chain. Life Cycle Assessment (LCAs) aids in comparing the environmental performance of different technologies, providing valuable insights for developing sustainable energy strategies.

While regional power collaborations and energy security efforts aim to enhance reliability and access to electricity, addressing the needs of poor households remains a challenge. Moreover, sustainable energy development requires considering environmental impacts comprehensively and integrating insights from LCA into energy planning. By addressing these challenges, policymakers can work towards achieving both energy security and sustainability goals.

The evaluation of the specific benefits of RE must consider country-specific contexts, particularly in developing nations where associated costs heavily influence the feasibility of RE adoption. Concerns have been raised about the potential impact of increased energy prices on the development prospects of industrializing countries. However, studies have shown that RE can offer cost savings, especially in poor rural areas without access to the grid.

1.2.1 Financial Barriers of Renewable Energy

Financial barriers to RE adoption remain a hot topic. For instance, global initiatives like the Copenhagen accord recognize the need for substantial financial

support for climate measures in developing countries[2].

The concept of Energy Payback Time (EPT) offers valuable insights into the energetic efficiency of electricity generation technologies, reflecting the balance between the energy invested in manufacturing, operating, and decommissioning the plants and their energy output. This metric, closely related to other indicators like Energy Return On Energy Invested (EROEI), sheds light on the sustainability and viability of different energy sources.

Over recent years, advancements in technology and economies of scale have led to declining EPTs for RE technologies such as wind and photovoltaic (PV). This trend underscores the potential for RE to become an increasingly competitive and sustainable alternative to conventional fossil and nuclear power.

Variability in estimates of EPTs is influenced by various factors, including fuel characteristics, cooling methods, uranium ore grades, material types, economies of scale, and storage capacity. Moreover, location-specific factors, notably the capacity factor, significantly affect EPT, particularly for variable RE technologies.

Understanding and minimizing EPTs are essential for transitioning towards more sustainable and efficient energy systems. By optimizing technological advancements, scaling up renewable energy deployment, and considering location-specific factors, the energy sector can work towards achieving shorter EPTs and enhancing the overall sustainability of electricity generation.

[2] https://unfccc.int/resource/docs/2009/cop15/eng/l07.pdf (Point 3)

Table 1 - Energy payback times and energy ratios of electricity generating technologies.[5]

Technology	Energy payback time (years)		Most commonly stated lifetime (years)	Energy ratio (kWh_e/kWh_{prim})	
	Low value	High value		Low value	High value
Brown coal, new subcritical	1.9	3.7	30	2.0	5.4
Black coal, new subcritical	0.5	3.6	30	2.5	20.0
Black coal, supercritical	1.0	2.6	30	2.9	10.1
Natural gas, open cycle	1.9	3.9	30	1.9	5.6
Natural gas, combined cycle	1.2	3.6	30	2.5	8.6
Heavy-water reactors	2.4	2.6	40	2.9	5.6
Light-water reactors	0.8	3.0	40	2.5	16.0
Photovoltaics	0.2	8.0	25	0.8	47.4
Concentrating solar	0.7	7.5	25	1.0	10.3
Geothermal	0.6	3.6	30	2.5	14.0
Wind turbines	0.1	1.5	25	5.0	40.0
Hydroelectricity	0.1	3.5	70	6.0	280.0

While substantial financial flows can support the transition to RE-based energy systems, proper governance of these funds is crucial to ensure they result in SD benefits and do not inadvertently hinder development. Lessons from the governance of resource rents and aid flows can inform best practices regarding transparency and revenue management.

Ultimately, the decision to adopt RE cannot be based solely on economic costs but must consider various factors, including ancillary benefits such as energy access, security, and environmental impacts, as well as potential funding opportunities through climate finance. This underscores the complexity of the decision-making process and the need for a holistic approach to energy planning.

Table 2 - Critical raw materials content of renewable resources technologies.[5]

Application	Component	Critical raw materials content
Wind and hydropower plants	Permanent magnets of synchronous generator	Neodymium, dysprosium, praseodymium, terbium
	Corrosion-resistant components	Chromium, nickel, molybdenum, manganese
Photovoltaics	Transparent electrode	Indium
	Thin film semiconductor	Indium, gallium, selenium, germanium, tellurium
	Dye-sensitized solar cell	Ruthenium, platinum, silver
	Electric contacts	Silver
Concentrating solar power (CSP)	Mirror	Silver
Fuel cell-driven electric vehicles	Hydrogen fuel cell	Platinum
	Electric motor	Neodymium, dysprosium, praseodymium, terbium, copper
Biomass to liquid (BtL)	Fischer-Tropsch synthesis	Cobalt, rhenium, platinum
Electricity storage	Redox flow rechargeable battery	Vanadium
	Lithium-ion rechargeable battery	Lithium, cobalt
Electricity grid	Low-loss high-temperature super-conductor cable	Bismuth, thallium, yttrium, barium, copper

Access to raw materials for future renewable resource deployment presents a challenge, particularly due to the scarcity of certain Inorganic mineral Raw Materials (IRMs). While renewable resources offer a promising avenue for mitigating fossil fuel depletion, the availability of the IRMs such as rare earth metals are crucial for their widespread deployment.

However, the structure and quantity of the IRMs demand in the RE sector have not been extensively assessed, highlighting a need for comprehensive analyses.

The IRMs supply chain is vulnerable to various threats, including concentration processes in major mining countries and political instability. China, for example, dominates the production of rare earth elements, while South Africa and Kazakhstan control a significant portion of the global chromium supply. Additionally, future IRMs constraints are expected to be driven more by imbalances in demand and supply rather than depletion of geological resources.

Certain metals, such as gallium and neodymium, are projected to experience significant increases in demand due to emerging technologies like thin-layer

photovoltaics and high-performance permanent magnets used in wind turbines and electric motors. However, the vulnerability of industrial sectors is heightened when there are no viable substitutes for essential raw materials as seen with chromium in stainless steels and cobalt in various applications.

Effective recycling systems are identified as crucial for ensuring a secure IRMs supply in the future. Implementing closed-loop recycling concepts from the outset of RE technology development could not only enhance supply security but also reduce dependency on primary supply sources and mitigate metal price volatility.

1.3 European Perspectives on Renewable Energy

December 2019, the European Commission introduced the European Green Deal, a comprehensive set of policy initiatives and strategies aiming to make the EU climate neutral by 2050, meaning that the EU's net greenhouse gas emissions will be reduced to zero by that year. The European Green Deal encompasses various sectors of the economy, including energy, industry, transportation, agriculture, and buildings, with the goal of achieving sustainability and environmental protection while fostering economic growth and social justice.

Key objectives of the European Green Deal include Climate Neutrality, Clean Energy Transition, Sustainable Industry, Sustainable Mobility, Biodiversity and Farm to Fork Strategy, Renovation Wave, Just Transition, Financing and

Investment.

The European Green Deal represents a comprehensive roadmap for the EU to transition to clean, affordable, and secure energy while meeting climate objectives for 2030 and 2050 within the European Union (EU).

Firstly, it emphasizes the critical need to prioritize energy efficiency across economic sectors, given that energy production and consumption contribute to over 75% of the EU's greenhouse gas emissions. To address this, the EU aims to develop a power sector primarily reliant on renewable sources, with a simultaneous phase-out of coal and decarbonization of gas. The integration, interconnection, and digitalization of the European energy market are highlighted as essential components to ensure security and affordability while respecting technological neutrality.

Member states are urged to present ambitious national contributions to EU-wide targets through revised energy and climate plans, which will be assessed by the Commission for adequacy.

Figure 3 - European Green Deal.[7]

Furthermore, this deal underscores the importance of consumer involvement and benefit in the clean energy transition, particularly through the utilization of renewable energy sources and increased offshore wind production. It emphasizes the smart integration of renewables, energy efficiency measures, and sustainable solutions across sectors to achieve decarbonization at minimal cost. Measures to address energy poverty, such as financing schemes for household renovations, are highlighted alongside the decarbonization of the gas sector and methane emission reduction efforts.

Additionally, this initiative delves into the necessity of smart infrastructure and increased cross-border cooperation to realize the benefits of the clean energy transition affordably. It advocates for a review of the regulatory framework for energy infrastructure to align with climate neutrality objectives, promoting the

deployment of innovative technologies and infrastructure like smart grids, hydrogen networks, and carbon capture, storage, and utilization.

Transitioning to a clean and circular economy is also emphasized, requiring full mobilization of industry. The deal highlights the urgency of action in the next five years to transform industrial sectors towards sustainability and circularity, reducing greenhouse gas emissions and reliance on resource extraction. Specific attention is drawn to energy-intensive industries like steel, chemicals, and cement, with recommendations for their decarbonization and modernization.

EU's plans to adopt an industrial strategy and a new circular economy action plan, emphasizing the role of digital transformation as a key enabler for reaching sustainability goals. It calls for measures to support the circular design of products, promote sustainable business models, and empower consumers to make informed choices.

To conclude, this set of policies underscores the comprehensive strategies and collaborative efforts required to achieve the EU's clean energy and climate objectives, emphasizing the importance of regulatory frameworks, industry mobilization, consumer involvement, and technological innovation.

1.4 Italian Perspective on Renewable Energy

Italy, as a net energy importer, relies on foreign energy sources, with imports constituting 80% of its Total Energy Supply (TES) between 2016 and 2021, predominantly oil and gas. Despite this dependency, Italy has made significant strides in renewable energy production. The primary domestic sources are bioenergy, hydro, solar, and wind, though the country produces a limited amount of oil and natural gas.

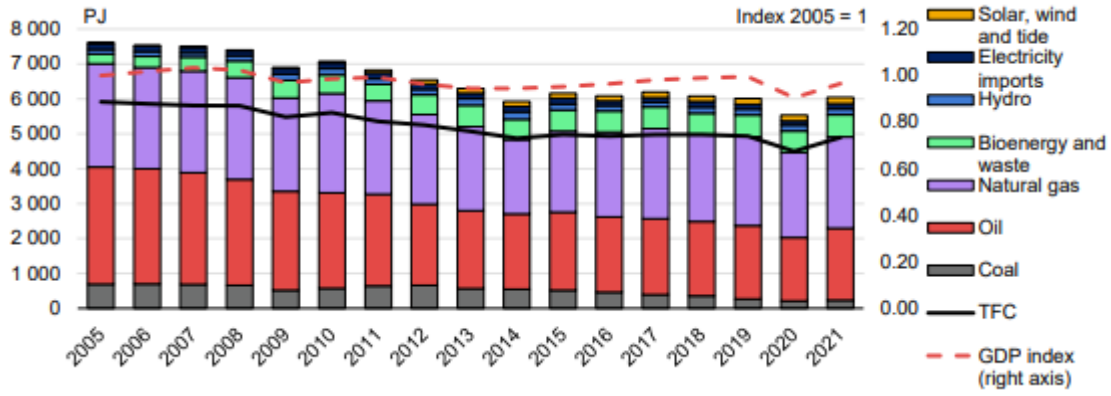

Figure 4 - Total energy supply by source, total final consumption, and GDP in Italy, 2005-2021.[8]

Natural gas plays a dominant role in Italy's electricity mix, accounting for 50% of total electricity generation in 2021, the second highest among International Energy Agency (IEA) countries.

Figure 5 - Map of Italy's gas infrastructure.[8]

Hydropower was the second-largest source at 16% followed by solar (9%), bioenergy and waste (8%), and wind (7%). Coal and oil contribute minimally to the energy mix.

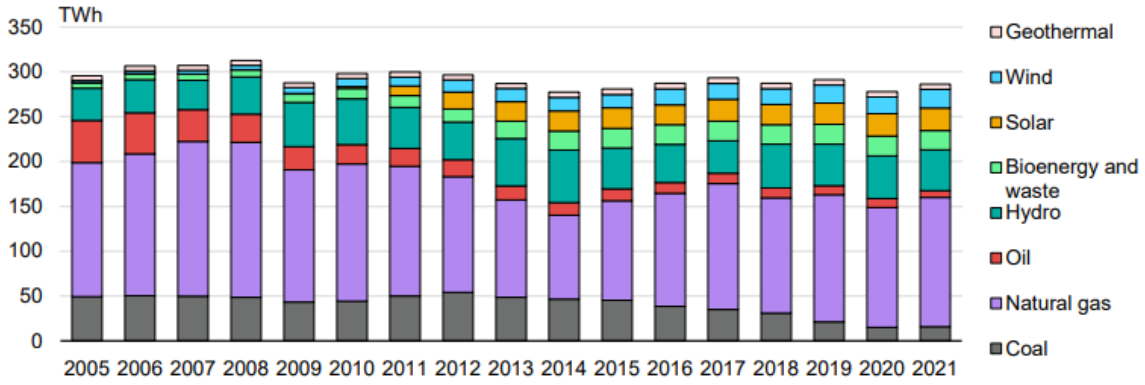

Figure 6 - Electricity generation by source in Italy, 2005-2021.[8]

		2020 status	2030 targets (NECP)	Expected or proposed targets 2030 (FF55)****
GHG emissions	**Net GHG emissions versus 1990 (including removals)**	-32%		-55%
GHG emissions covered by the Effort Sharing Regulation*	**CO_2-eq emissions versus 2005**	-25%	-33%	-43.7%
Energy efficiency	**Primary energy consumption**	6 084 PJ (2021)	5 238 PJ	4 681 PJ
	Final energy consumption	4 742 PJ (2021)	4 346 PJ	3 936 PJ
Renewable energy share (in gross final energy consumption)**	**Overall target**	19.0% (2021)	30%	36.7%
	Electricity	36.0% (2021)	55.4%	62-65%
	Heating and cooling	19.7% (2021)	33.9%	40%
	Transport	10.0% (2021)	21.6%	38%
Renewable electricity in total electricity generation (ETP target)				72%
Cross-border electricity interconnection***		8%	10%	
Energy dependence		77.7% (in 2016)	75.4%	

Table 3 – Italy's 2030 energy and climate targets.[8]

According to the EU's energy and climate policy framework, Italy aims to decarbonize its energy supply through the expansion of renewable energy, electrification, and increased energy efficiency. This strategy is consistent with the IEA roadmap to net zero emissions by 2050. However, recent geopolitical events, particularly Russia's invasion of Ukraine, have refocused Italy's political

attention on energy security, leading to an announcement that it will cease importing Russian gas by 2025.

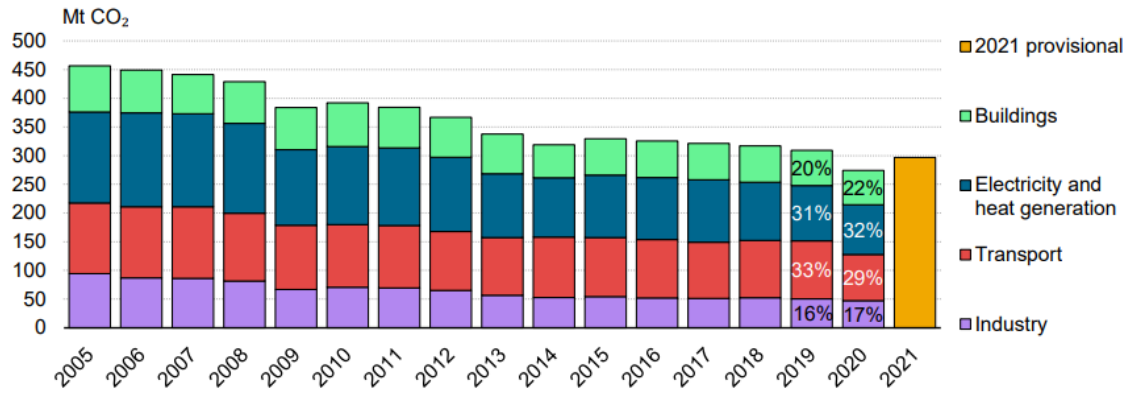

Figure 7 - Energy-related CO2 emissions by sector in Italy, 2005-2021.[8]

Italy's National Plan for the Containment of Natural Gas Consumption, issued in September 2022, is part of its broader strategy to enhance energy security while striving for decarbonization. The government also plans to ban coal use for electricity production by 2025, contingent on developing adequate replacement capacity and ensuring grid stability.

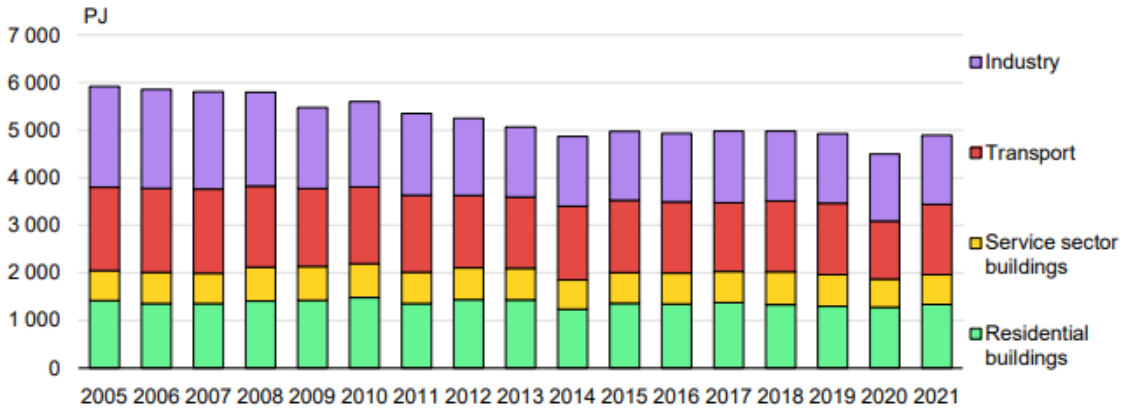

Figure 8 - Total final consumption by sector in Italy, 2005-2021.[8]

The National Energy and Climate Plan (NECP) sets ambitious targets for renewable energy, aiming to reach 30% of gross energy consumption from renewables by 2030. Achieving these targets will require significant scaling up of renewable energy production and improvements in energy efficiency. The IEA suggests that adding 2 GW of renewables annually could reduce Italy's dependence on Russian gas by 1% each year.

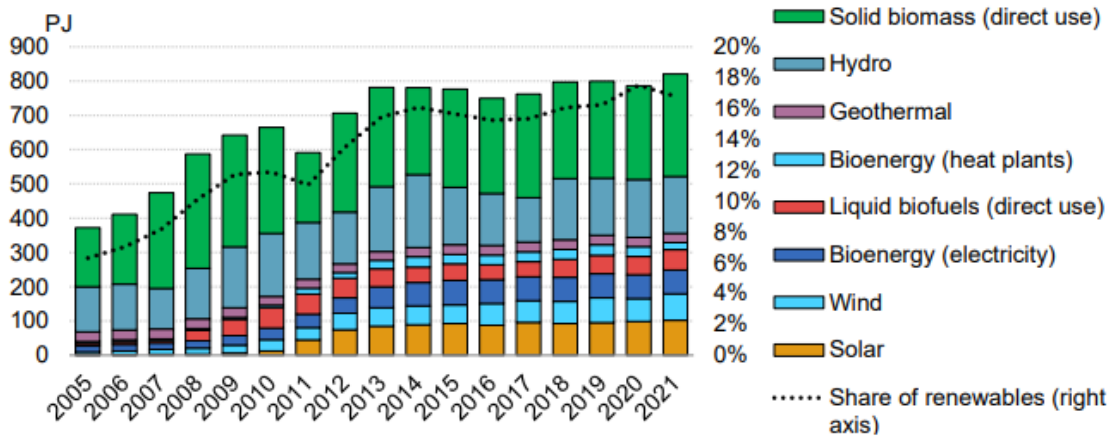

Figure 9 - Renewable energy in total final energy consumption in Italy, 2005-2021.[8]

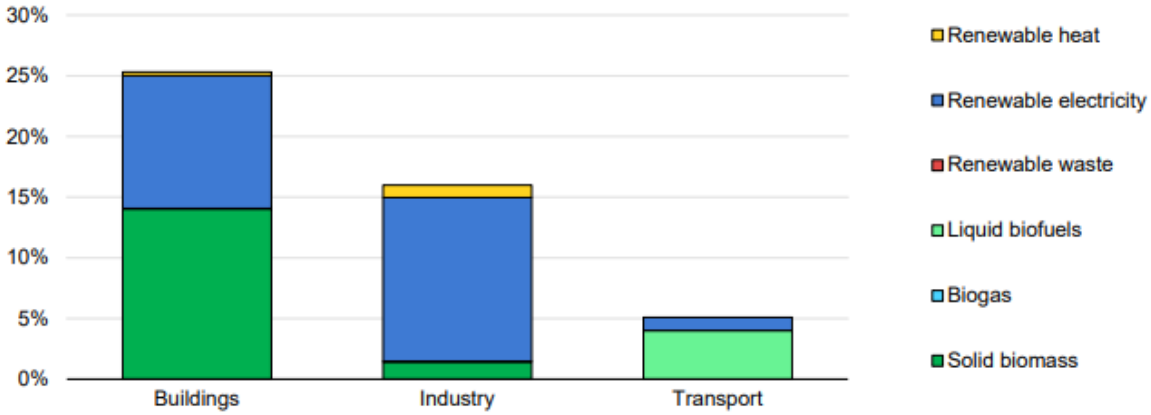

Figure 10 - Share of renewables by end-use sector and source in Italy, 2021.[8]

Italy's RE use has grown substantially over the past decade, but recent years have seen a slowdown in deployment due to the phasing out of incentives, long permitting procedures, and high administrative burdens. RE accounted for 20.4% of gross final energy consumption in 2020, exceeding the EU target of 17%. Bioenergy remains the largest renewable source, followed by hydropower, which is susceptible to variability due to climate conditions.

The NECP focuses on expanding wind and solar power, developing offshore multipower systems, and promoting energy communities and agrivoltaics. It also emphasizes the production and use of biomethane. The National Recovery and Resilience Plan (NRRP) allocates significant funding to support renewable energy projects and grid upgrades.

Electricity generation from renewable sources more than doubled from 2005 to 2021, reaching 40.5% of total electricity generation. However, growth has been uneven across regions, with the north favouring non-variable sources like hydro and bioenergy, while the south relies more on variable sources like solar and wind. This regional disparity complicates the management of electricity flows and requires significant investment in grid infrastructure.

The government has introduced measures to simplify and expedite permitting processes for renewable projects and grid developments. Legislative Decree 199/2021, implementing the EU Renewable Energy Directive (RED II), aims to streamline administrative procedures and enhance investment incentives.

Looking forward, Italy's energy transition will necessitate substantial investment in grid infrastructure to accommodate the increasing share of variable renewable energy. The NECP projects a need for 95 GW of RE capacity by 2030, a significant increase from current levels. Achieving these targets will require overcoming administrative barriers, engaging local stakeholders, and ensuring a just transition that addresses energy poverty.

CHAPTER 2 - HYDROGEN AS A TRANSFORMATIVE ENERGY CARRIER

Hydrogen, often seen as the fuel of the future, holds immense potential as a transformative energy carrier in the quest for sustainable energy solutions. Its versatility and potential for decarbonization make it a key player in the transition towards cleaner and more efficient energy systems.

Hydrogen finds applications both as a direct fuel and as an energy carrier. It can be used directly by blending with natural gas or in fuel cells for electricity generation. Its high energy density makes it an attractive option for various applications, including transportation, industrial processes, and energy storage systems. However, its low volumetric energy density poses challenges for storage and distribution, requiring innovative solutions.

From an environmental perspective, hydrogen production from Renewable Energy Sources (RES), or in combination with Carbon Capture and Storage (CCS), contributes to decarbonization efforts by reducing greenhouse gas emissions associated with conventional fossil fuels. However, challenges remain in scaling up renewable hydrogen production and ensuring its cost-effectiveness compared to fossil fuel-based hydrogen.

Several countries are already making significant steps in developing hydrogen economies with initiatives ranging from pilot projects to large-scale deployment of hydrogen infrastructure. Countries like Japan, Germany, and South Korea are leading the way in hydrogen technology innovation and investment, paving the

path for others.

Hydrogen holds immense promise as a transformative energy carrier with the potential to revolutionize energy systems and drive sustainable development. By leveraging its unique properties and addressing existing challenges, hydrogen can play a crucial role in achieving global climate goals and building a cleaner, more resilient energy future. However, efforts and investments are needed to overcome barriers and unlock the full potential of hydrogen as a key player in the transition towards a low-carbon economy.

2.1 The Significance of Hydrogen

Hydrogen is experiencing an increase in interest, particularly in Europe. Its versatile nature as a feedstock, fuel, and energy carrier makes it indispensable across various sectors such as industry, transportation, power generation, and buildings.

Despite its potential, hydrogen currently constitutes only a small fraction of the global and European energy mix, primarily produced from fossil fuels like natural gas and coal, resulting in significant CO_2 emissions. To realize its potential as a climate-neutral energy carrier, hydrogen production must undergo a transformative shift towards decarbonization. Fortunately, recent advancements in technology, coupled with the declining costs of renewable energy, are creating new opportunities for hydrogen.

The momentum surrounding hydrogen is evident, with increasing investments

and growing participation from companies and organizations globally. The European Union (EU) recognizes the role of hydrogen in achieving its ambitious climate goals, with projections indicating a significant increase in its share in the energy mix by 2050. Renewable hydrogen, produced through electrolysis powered by renewable energy sources, is expected to play a crucial role in bridging the gap towards climate neutrality.

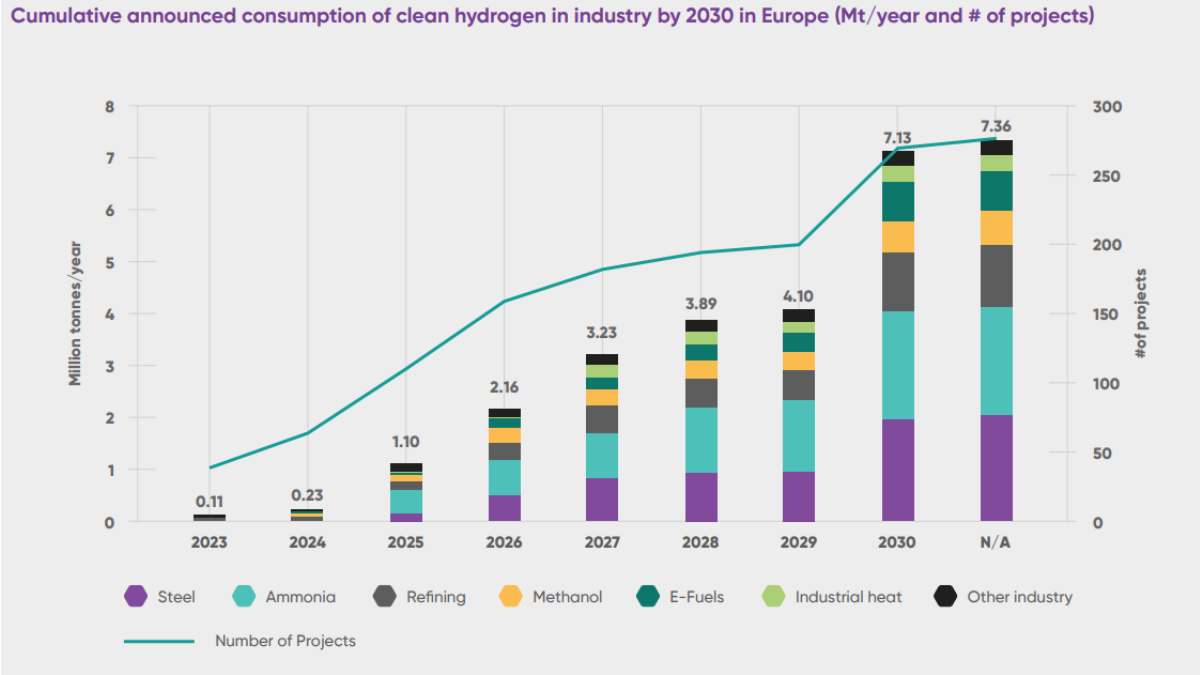

Figure 11 - Cumulative announced consumption of hydrogen in industry by 2030 in Europe.[9]

Hydrogen's potential to replace fossil fuels in carbon-intensive industries like steel and chemicals further enhances its importance in the transition to a low-carbon economy. Moreover, hydrogen can leverage existing natural gas infrastructure, minimizing stranded assets and facilitating a smoother transition. The EU's strategic roadmap for hydrogen outlines ambitious targets, including the installation of renewable hydrogen electrolysers and the production of

millions of tonnes of renewable hydrogen by 2030. This roadmap envisions a gradual transition towards renewable hydrogen, supported by policy frameworks, investments, and collaborative efforts across sectors. It emphasizes the need for regulatory support, infrastructure development, and market incentives to drive the hydrogen ecosystem's growth.

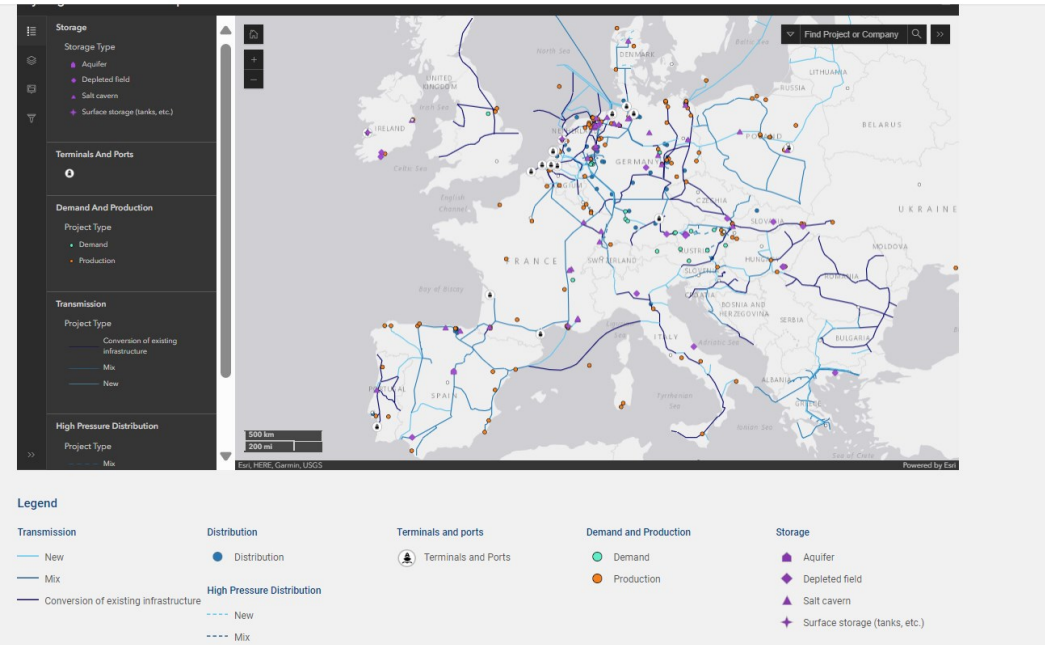

Figure 12 - Hydrogen transportation projects in Europe [10]

In the short term, the focus is on scaling up renewable hydrogen production and decarbonizing existing hydrogen production through retrofitting and carbon capture technologies. This phase involves laying down the groundwork for a well-functioning hydrogen market, incentivizing supply and demand, and fostering innovation and investment. As renewable hydrogen becomes cost-competitive, it will progressively replace fossil-based hydrogen leading to a more sustainable energy system.

Looking ahead to 2030 and beyond, hydrogen is poised to become an integral

part of an integrated energy system offering flexibility, storage, and balancing capabilities. Local hydrogen clusters, or "Hydrogen Valleys," will emerge by leveraging decentralized RESs to meet local demand and provide heating solutions for residential and commercial buildings.

REPowerEU Plan aims to reduce dependence on Russian fossil fuels and accelerate the green transition. As part of this initiative, a target of 10 million tonnes of domestic renewable hydrogen production and 10 million tonnes of imports by 2030 has been set.

In conclusion, hydrogen's importance in the transition to a low-carbon economy cannot be overstated. It offers a viable pathway to decarbonize hard-to-abate sectors and facilitate the integration of renewable energy sources. With strategic planning, investment, and collaboration, hydrogen has the potential to revolutionize the energy landscape and contribute significantly to achieving climate neutrality and a sustainable future.

2.2 Usage of Hydrogen

Hydrogen is emerging as a crucial component in the transition to a low-carbon energy system serving both as a fuel for electricity production and a medium for energy storage. The versatility of hydrogen lies in its ability to be produced from various sources, including renewable energy, and its potential to decarbonize sectors where electrification is challenging.

Hydrogen can be used directly as a fuel in fuel cells or burned in gas turbines to

produce electricity. It is environmentally friendly option for electricity generation. Hydrogen turbines, meanwhile, can be adapted from existing natural gas turbines, providing a flexible and scalable solution for integrating hydrogen into the power sector.

Hydrogen also plays a significant role in energy storage by addressing the intermittency of renewable energy sources. Excess electricity generated during periods of high renewable output can be used to produce hydrogen via electrolysis. This hydrogen can be then stored and converted back into electricity when demand exceeds supply or renewable generation is low. This process, known as Power-to-Gas-to-Power (P2G2P), enhances grid stability and ensures a continuous energy supply.

2.2.1 Hydrogen for decarbonizing transport

The Roundtable Mobility, held in Brussels on 29 February 2024 by the European Commission, was an event focused on the transition pathway for the mobility ecosystem. It has extensively deliberated on the challenges and opportunities surrounding the integration of hydrogen in the transport sector. Through collaborative discussions among its members, various barriers hindering the development of the hydrogen ecosystem in transportation have been identified.

One of the primary challenges facing the hydrogen ecosystem is the lack of standardized regulations and procedures. To unlock the market potential, standardization efforts must be intensified. Key challenges and mitigation

measures in this regard include:

a) Establishing clear definitions and standards for certifying low carbon and green hydrogen by ensuring differentiation between locally produced and imported hydrogen.
b) Implementing an exchange for green hydrogen to establish a reference price and certification system for carbon capture and reuse.
c) Developing international standards for vehicle on-board hydrogen storage, safe integration of hydrogen propulsion systems, and refuelling infrastructure.

Standardization and infrastructure availability are critical for ecosystem development. Additional regulatory measures are needed to address challenges such as integrating externalities in transport cost structures and increasing the share of renewables in all transport modes. Mitigation measures include:

a) Establishing an adjacent emissions trading system for road transport to internalize carbon costs.
b) Implementing strict sustainability criteria for sustainable aviation fuel and revising the Renewable Energy Directive (RED) to stimulate supply in the transport sector.
c) Ensuring a coherent regulatory framework for maritime hydrogen applications and incentivizing hydrogen propulsion technology in aviation.

Hydrogen fuel-cell trains and busses are highlighted as a viable alternative for difficult-to-electrify routes, with certain applications already cost competitive with diesel.

Hydrogen can power vehicles through fuel cells or Internal Combustion Engines (H_2 ICE). Fuel cells generate electricity from onboard board hydrogen, while H_2 ICE directly combusts hydrogen, emitting lower CO_2 emissions.

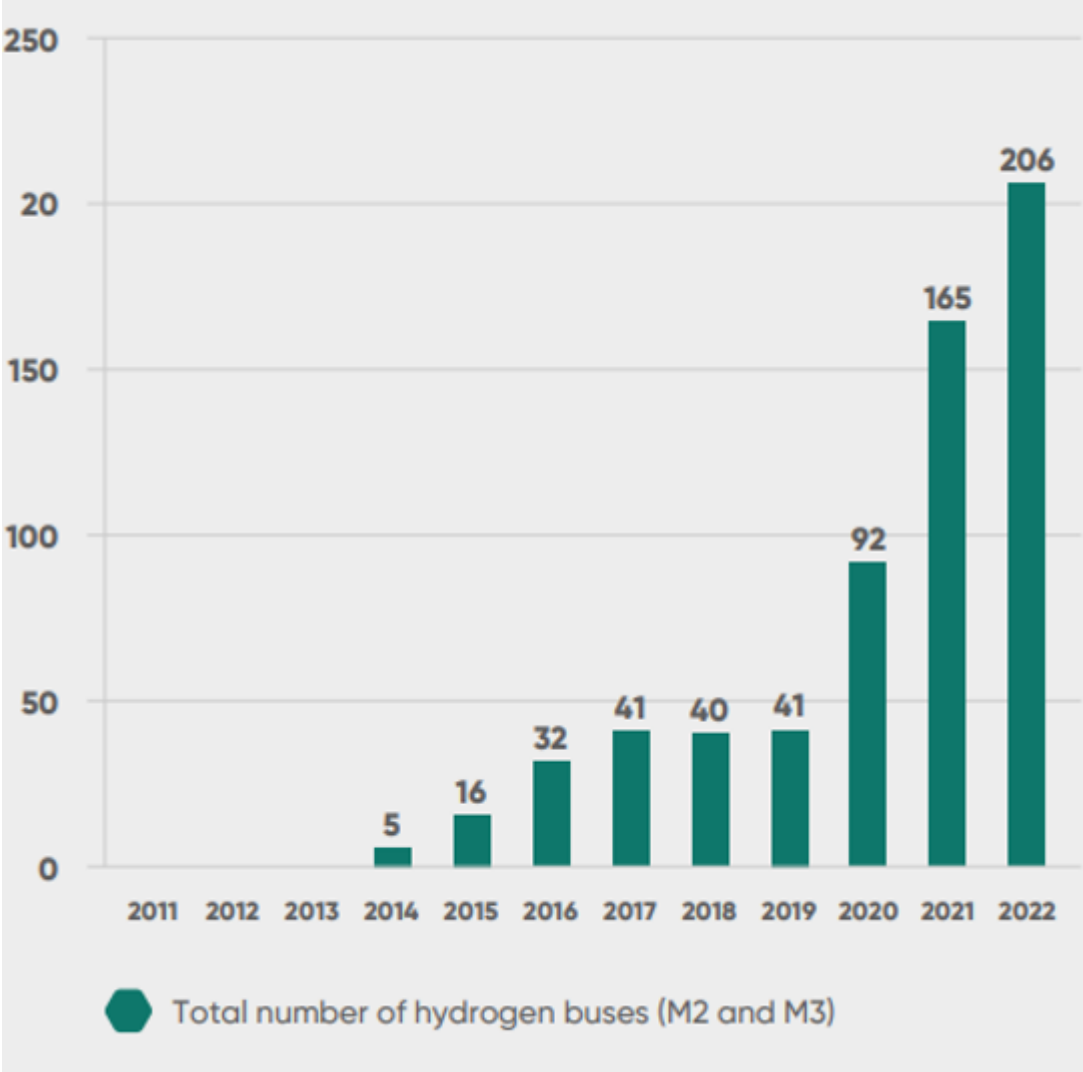

Figure 13 - Number of hydrogen-powered busses in Europe.[9]

Hydrogen can be stored as gas or liquid, with different pressure levels suitable for various vehicle types. Gaseous hydrogen at 350 or 700 bar is used for heavy-duty trucks and personal vehicles, while Liquid Hydrogen (LH_2) is suitable for heavy-duty applications.

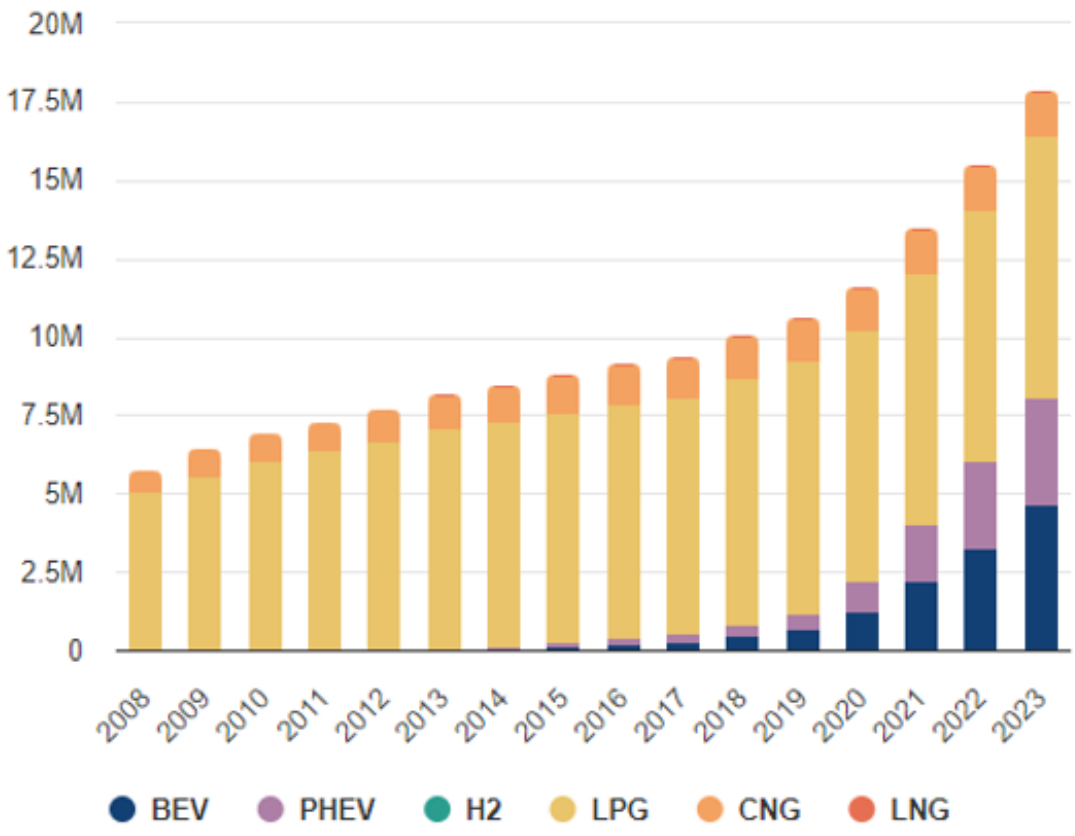

Figure 14 - Total number of alternative fuelled (BEV, PHEV, H2, LPG, CNG, LNG) passenger cars (M1) and vans (N1) in EU. [9]

In the personal vehicle market, hydrogen adoption is gradual with limited models available. However, manufacturers are expanding offerings, with steady growth anticipated. Light-Duty Vehicles (LDVs) and buses show similar trends, with hydrogen-powered variants offering advantages like longer range and quick refuelling.

In the maritime sector, decarbonization targets are set under regulations like FuelEU Maritime. Hydrogen, alongside other fuels like methanol and ammonia, holds promise for reducing emissions.

Despite challenges, hydrogen holds significant potential for decarbonizing the

transportation sector, particularly in heavy-duty applications. Cost reduction through research, development, and infrastructure investment is crucial for realizing hydrogen's full potential and achieving sustainable mobility.

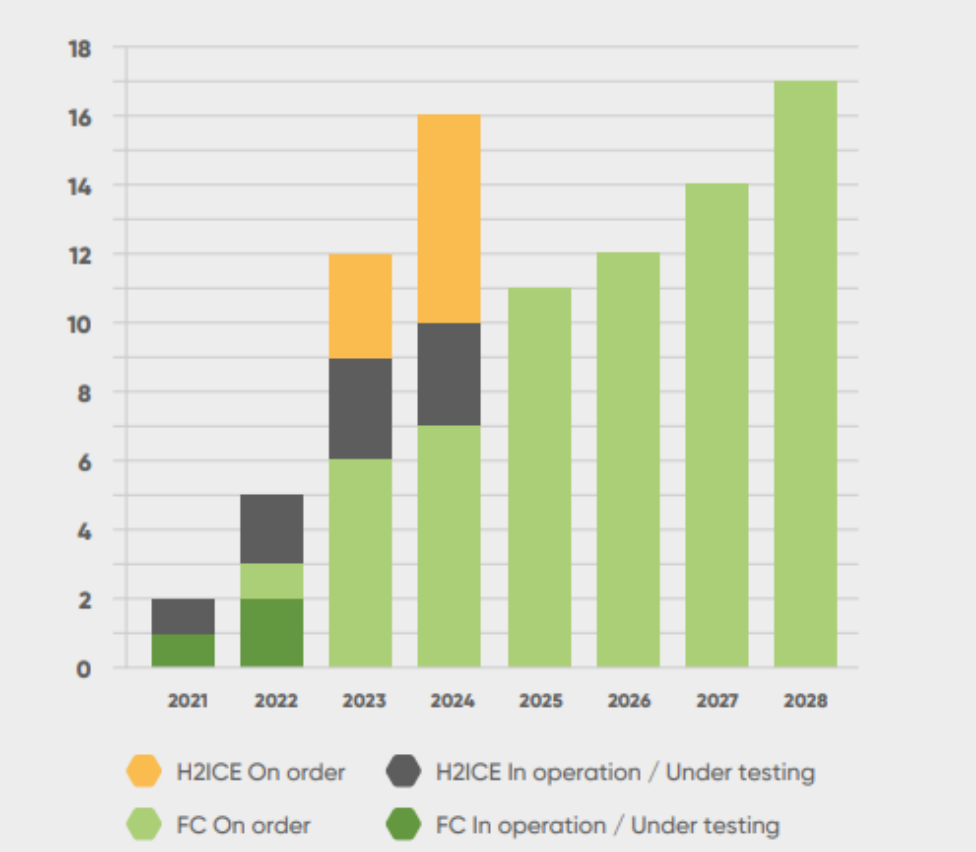

Figure 15 - Number of hydrogen fuel cells and ICE ships per year of delivery.[9]

Sea shipping could benefit from hydrogen as a low-emission fuel, especially with increasing emphasis on pricing CO_2 emissions in the maritime sector.

2.2.2 Hydrogen for clean heating systems

Despite the growing momentum towards decarbonization, consumers remain largely unaware of the pathway to utilizing hydrogen-methane blends for heating.

Existing regulations often favour electrification over hydrogen integration in building heating systems. Moreover, limited consumer awareness of hydrogen-readiness impedes demand for hydrogen-ready technologies. Regulatory reforms are imperative to promote technological openness and establish EU targets for renewable gases. Adaptation of gas appliance regulations to accommodate hydrogen usage is essential for fostering market readiness.

Insecure funding environments and biases towards conventional technologies hinder investments in hydrogen-ready building solutions. Shifting from CAPital EXpenditure (CAPEX) to OPerational EXpenditure (OPEX) support can bridge the cost gap and attract positive financing. Promoting building technologies as hydrogen-ready and broadening funding allocations can further accelerate adoption.

Low awareness of hydrogen-ready heating technologies and time-consuming certification processes pose significant barriers. Raising awareness through large-scale demonstration projects and focusing on cost reduction and efficiency improvements are vital. Streamlining certification and standardization processes is essential for expediting commercialization and widespread adoption.

Synchronization across the hydrogen supply chain is critical for seamless integration into the building sector. Robust European and global supply chains, along with investments in workforce upskilling, are necessary for ensuring reliable sourcing and installation of hydrogen-ready infrastructure.

The roundtable meetings focused on energy efficient buildings highlight the transformative potential of hydrogen-methane blends in the heating sector. By addressing barriers and implementing mitigation measures across market, regulatory, funding, technology, and supply chain domains, the building sector can embrace sustainable heating solutions and contribute significantly to the broader clean energy transition. Collaboration and concerted efforts among stakeholders are essential for realizing this vision and creating a more resilient and sustainable built environment.

As the European Clean Hydrogen Alliance (ECH$_2$A) emphasizes the importance of hydrogen imports, it becomes imperative to address the challenges hindering the development of hydrogen infrastructure.

Establishing strategic partnerships between the EU and exporting countries is paramount for ensuring a reliable supply of hydrogen. However, differing standards and certification processes pose a significant challenge. Harmonizing certification standards globally is essential to facilitate trade and ensure the integrity of hydrogen as a sustainable energy source.

2.2.3 Hydrogen for energy storage and electricity production

Green hydrogen, produced via the electrolysis of water using renewable energy sources such as wind, solar, and hydropower, is emerging as a key solution for both energy storage and electricity production.

One of the most promising applications of green hydrogen is in energy storage, particularly through the P2G technology. In this process, surplus electricity from RESs is used to produce hydrogen via electrolysis. This hydrogen can be stored and later converted back into electricity or used in other applications.

Green hydrogen offers an effective solution for long-term energy storage by addressing the intermittency of RESs. Unlike batteries, which are suitable for short to medium-term storage, hydrogen can store energy over weeks or months, ensuring a continuous energy supply.

By converting excess RE into hydrogen, green hydrogen helps stabilize the electricity grid by preventing curtailment of renewable energy and balancing supply and demand.

Hydrogen fuel cells on the other hand are a crucial technology for electricity production. They generate electricity through a chemical reaction between hydrogen and oxygen, with water and heat as the only by-products. This process is highly efficient and produces no greenhouse gas emissions at the point of use.

Hydrogen can also be used in Combined Heat and Power systems (CHP) to generate both electricity and heat. These systems are particularly beneficial in industrial and residential applications, improving overall energy efficiency.

The use of green hydrogen significantly reduces carbon emissions in both electricity production and storage, contributing to climate change mitigation efforts.

Green hydrogen enhances energy security by diversifying energy sources and reducing dependence on fossil fuels. It can be produced locally from abundant renewable resources, minimizing geopolitical risks associated with energy imports. Furthermore, developing green hydrogen infrastructure and technologies can stimulate economic growth, create jobs, and drive innovation in the energy sector.

Green hydrogen holds immense potential for revolutionizing energy storage and electricity production. By harnessing renewable energy sources to produce hydrogen, it offers a sustainable, efficient, and flexible solution to some of the most pressing challenges in the energy sector. While significant hurdles remain, continued innovation, supportive policies, and collaborative efforts are paving the way for green hydrogen to become a cornerstone of the global energy transition.

2.4 Progress of Hydrogen in Italy

Italy has significantly increased its focus on hydrogen development in recent years, driven by both decarbonization goals and the need for energy security, especially considering the natural gas crisis exacerbated by Russia's invasion of Ukraine. This dual focus underscores hydrogen's potential as a clean energy source and a secure energy carrier.

In 2020, the Ministry for the Ecological Transition (MiTE) released preliminary

hydrogen guidelines (Strategia Nazionale Idrogeno: Linee Guida Preliminari) to pave the way for a comprehensive national hydrogen strategy. These guidelines aim to replace up to 2% of natural gas with hydrogen by 2030 and project hydrogen to account for 2% of Final Energy Consumption (FEC) by the same year, potentially reducing CO_2 emissions by 8 million tonnes. By 2050, hydrogen could contribute 20% to FEC, saving an estimated 97 million tonnes of CO_2. The Long-Term Strategy (LTS) integrates hydrogen into its decarbonization framework, emphasizing its role in transportation, synthetic fuel production, and hard-to-abate industrial sectors with some use in building heating systems.

Table 4 - Hydrogen-related investment in Italy's National Resilience and Recovery Plan

Projects	Allocation of public funds (EUR billion)	Expected outcomes
Hydrogen use in hard-to-abate industry (refinery and steel)	2	Decarbonise at least one industrial plant
Production of green hydrogen in brownfield sites (hydrogen valleys)	0.5	10 projects of renewable electricity plants to produce hydrogen, with capacity of 1-5 MW each
Hydrogen production plant	0.45	1 large electrolysis plant, with a capacity of 1 GW
Piloting hydrogen use in road transport	0.3	9 refuelling stations for trains along 6 non-electrified railway lines
Piloting hydrogen use in road transport	0.23	40 refuelling stations on highways, logistic terminals and ports
Research and development	0.16	At least 4 research projects on production, storage and distribution of hydrogen

Italy has invested in hydrogen Research and Development (R&D) and participates in international projects such as Important Projects of Common European Interest and Mission Innovation. These efforts are crucial for advancing hydrogen technologies and fostering innovation. Additionally, the National Recovery and Resilience Plan (NRRP) allocates EUR 3.6 billion for hydrogen rollout by 2026, aiming to bridge regulatory gaps and promote technical safety standards, administrative procedures for hydrogen production plants and refuelling stations, and a system of guarantee of origin.

Short-term strategies focus on deploying hydrogen in the transport sector, particularly for long-haul freight and non-electrified railways, and in industrial sectors where hydrogen is already used as feedstock. The government plans to install 5 GW of electrolysis capacity by 2030 to meet the rising demand for hydrogen. Italy's ambition includes covering 5-7% of domestic road fuel demand with hydrogen by 2030, with a particular focus on railways where diesel use remains prevalent.

Despite the strategic plans, Italy faces challenges related to the high costs of hydrogen production and infrastructure development. Access to low-cost renewable electricity is critical for reducing hydrogen costs. Preliminary modelling by RSE (Ricerca sul Sistema Energetico) suggests that achieving the EU Fit-For-55 (FF55) targets would require 0.63 million tonnes of oil equivalent (Mtoe) of renewable-based hydrogen by 2030, necessitating around 9 TWh of renewable electricity or 5-7 GW of additional renewable capacity.

The gas transmission system operator, SNAM, has piloted hydrogen-natural gas

blending and reports that 70% of its gas network is compatible with hydrogen transport. However, the high costs of hydrogen transport and storage, compared to other fuels like biomethane, and limited storage facilities pose significant challenges. It appears more cost-effective to prioritize hydrogen use in industry, locating production plants close to industrial facilities and transporting the necessary renewable electricity via the grid.

Italy aims to leverage its robust gas network and interconnections to become a European hydrogen hub, acting as a "bridge" between Europe and North Africa, where hydrogen can be produced from solar energy at lower costs. This vision includes the progressive reconversion of natural gas infrastructures for hydrogen transport and distribution, moving towards pure hydrogen transport in the future. Overall, Italy's commitment to hydrogen development is clear with substantial investments and strategic planning in place. Success will depend on overcoming economic and infrastructural challenges, fostering international collaboration, and ensuring policy support to realize hydrogen's potential in Italy's energy.

CHAPTER 3 – HYDROGEN PRODUCTION

One of the primary methods of hydrogen production is through Steam Methane Reforming (SMR) or methane pyrolysis processes, which extract hydrogen from natural gas. Often referred to as 'Fossil-based hydrogen' represents the bulk of hydrogen produced today. Currently, SMR remains the most common method due to its efficiency and widespread availability. The greenhouse gas emissions of the production of fossil-based hydrogen are high, but integration with carbon capture has lower emissions.

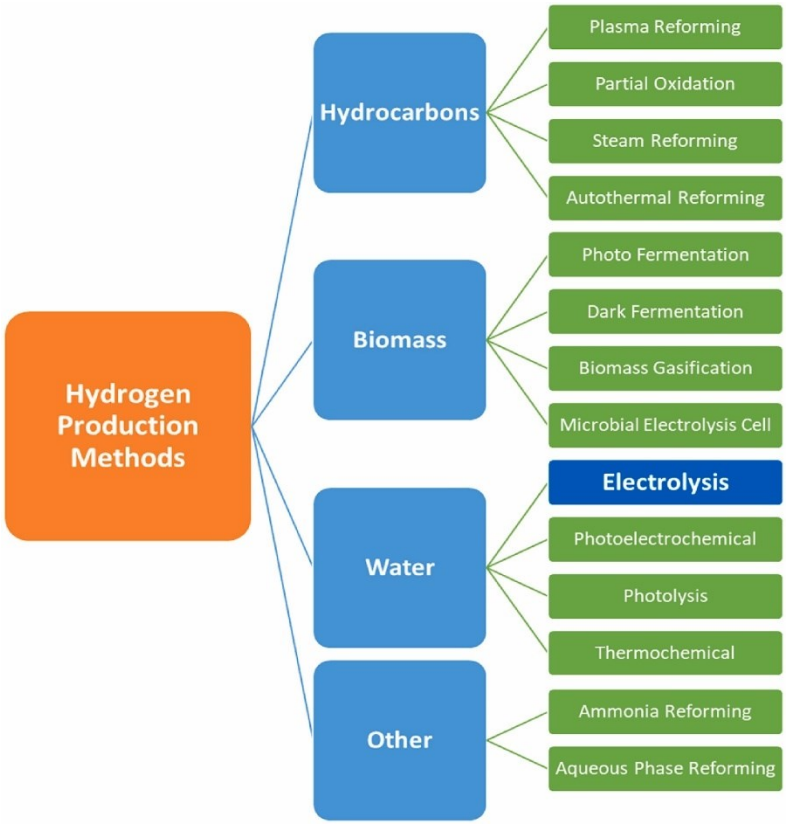

Figure 16 - Hydrogen production methods.[11]

Table 5 - An overall range for cost, efficiency, CO2 footprint, and color terminology for most common hydrogen production methods.[11]

Method	Description	Cost of Hydrogen ($/kg)	Efficiency	CO_2 Footprint (kg CO_2/kg H2)	Colour Terminology
Steam Methane Reforming (SMR)	The most common method for producing hydrogen, in which methane (natural gas) is reacted with steam to produce hydrogen and carbon dioxide.	$1.00–$2.50	65–75%	1.20–1.80	Grey hydrogen
Electrolysis of water	It is a technique that uses direct electric current to chemically split water into H2 and O2 gases.	$2.00–$6.00	60–90%	Depends on source of electricity	Green hydrogen
Gasification	Involves converting carbon-containing materials such as coal, biomass, or waste into a mixture of hydrogen and carbon monoxide through partial oxidation.	$2.00–$6.00	50–80%	1.50–2.50	Brown hydrogen
Fermentation	Microorganisms can be used to ferment organic matter, producing hydrogen as a byproduct.	$5.00–$7.00	40–50%	0.10–0.20	Bio hydrogen
Photobiological production	Certain microorganisms can use light to produce hydrogen through a process called photobiological hydrogen production.	$7.00–$10.00	30–40%	0.05–0.10	Blue hydrogen

Additionally, electrolysis, known as power-to-gas, splits water into hydrogen and oxygen using electricity. The full life-cycle greenhouse gas emissions of the

production of electricity-based hydrogen depends on how the electricity is produced.

Gasification processes can also convert solid fuels like coal or biomass into hydrogen, while anaerobic digestion can produce hydrogen from wet biomass.

3.1 Electrolysis

Electrolysis is a key technology for producing green hydrogen, which is hydrogen generated using renewable energy sources and water as feedstock. This process involves the splitting of water molecules (H_2O) into hydrogen (H_2) and oxygen (O_2) gases through the application of an electrical current. Electrolysis plays a crucial role in the production of green hydrogen as it offers a clean and sustainable method for generating hydrogen without producing greenhouse gas emissions.

Electrolysis operates based on the principle of electrochemical reactions occurring at electrodes immersed in an electrolyte solution. When an electric current is passed through the electrolyte, it induces chemical reactions that result in the decomposition of water into its constituent elements.

Electrolysis occurs in an electrolytic cell, a specialized electrochemical cell that converts electrical energy into the chemical one required for the process. This cell consists of two metal electrodes immersed in an electrolytic solution and connected to an electrical power source. When an electric field is applied, free ions in the electrolyte move: positive ions (cations) head toward the negative

electrode (cathode), and negative ions (anions) move toward the positive electrode (anode). Upon reaching the electrodes, cations gain electrons at the cathode (reduction), while anions lose electrons at the anode (oxidation). These simultaneous oxidation-reduction reactions at the electrodes constitute the overall electrolysis process.

A key characteristic of electrolysis is the direct relationship between the electrical current supplied and the amount of substance produced or consumed. This relationship is described by Faraday's law of electrolysis, which states that the quantity of product formed, or reactant consumed is proportional to the number of electrons exchanged.

An electrolytic cell is composed of:

- Two electrodes
- An electrolyte
- A separator (or diaphragm).

The separator divides the cell into two sections, preventing the mixing of generated hydrogen and oxygen gases while allowing ion passage between the cathode and anode. Multiple electrolytic cells arranged in series within a container form an electrolyser.

3.2 Types of electrolysers

Main types of electrolyzers are Proton Exchange Membrane (PEM), Alkaline

Water Electrolysis (AWE), Anion Exchange Membrane (AEM), Solid Oxide Electrolysis (SOE). They differ on the type of the operating temperature and other conditions. Further details will be discussed below for each type of technology.

3.2.1 Proton Exchange Membrane (PEM) electrolyser

In PEM electrolysis, an electrolyte membrane selectively allows the passage of protons (H^+) while blocking the passage of other ions. This type of electrolysis operates at relatively low temperatures (typically below 100°C) and is suitable for small-scale applications and integration with renewable energy sources such as solar and wind power.

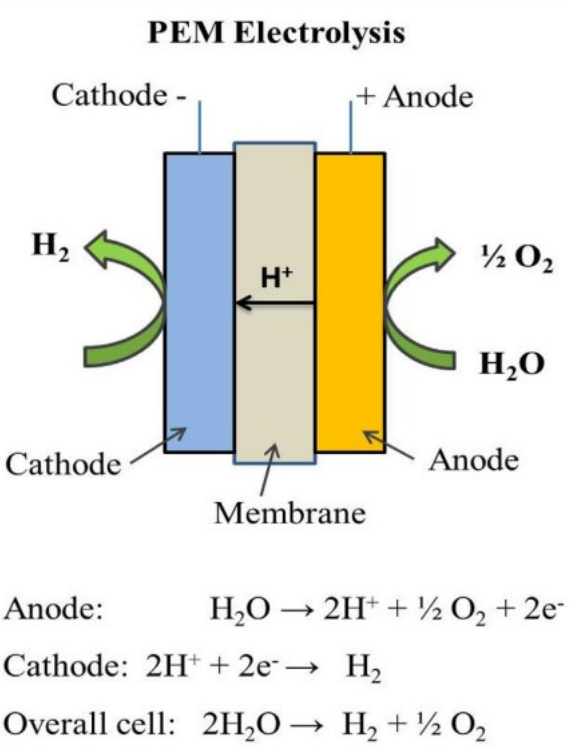

Figure 17 - Schematic illustration of PEM water electrolysis.[12]

In PEM water electrolysis, water molecules undergo electrochemical splitting

into hydrogen and oxygen at their respective electrodes. Hydrogen is produced at the cathode, while oxygen is produced at the anode. Water is pumped to the anode, where it is split into oxygen, protons, and electrons. Protons travel through a proton-conducting membrane to the cathode, while electrons exit the anode through an external circuit, by providing the driving force for the reaction.

The minimum energy required for water splitting is calculated using Gibbs free energy (ΔG). The reversible voltage (E_{rev}) required for the process is determined based on ΔG. Additionally, enthalpy (ΔH) is considered for potential calculation, considering entropy generated during water splitting.

$$\boldsymbol{\Delta G = nFE_{rev}} \qquad (1)$$

where:

n - no. of electrons involved

F - 96500 (Faraday's constant)

E_{rev} - Reversible voltage

The reversible voltage can be calculated as:

$$\boldsymbol{E_{rev} = \frac{\Delta G}{nF} = 1.23V} \qquad (2)$$

However, at the time of water splitting some entropy is generated. Thus, it is more suitable to employ enthalpy (ΔH) in its place of ΔG for the potential calculation. Therefore, at the standard conditions, the change of enthalpy is ΔH

= 285.84 kJ/mol and change of Gibbs free enthalpy is ΔG = 237.22 kJ/mol. Therefore, the minimum required voltage (V_{TN}) for the water electrolysis can be calculated by following Equation:

$$\boldsymbol{V_{TN} = \frac{\Delta H}{nF} = \frac{\Delta G}{nF} + \frac{T\Delta S}{nF} = 1.48V} \qquad (3)$$

V_{TN} = thermo-neutral voltage

ΔS = change in entropy

T = temperature

$$\boldsymbol{\eta = \frac{V_{TN}}{V_{cell}}} \qquad (4)$$

where:

V_{TN} - Thermo-neutral voltage

V_{cell} - Cell voltage

The efficiency of water electrolysis is calculated by comparing the theoretical minimum voltage (V_{TN}) required for the process with the actual cell voltage. Higher efficiency is achieved at lower current densities and voltages.

$$\boldsymbol{\eta_{Faraday} = \frac{V_{H2\_Produced}}{V_{H2\_Calculated}}} \qquad (5)$$

Faradaic efficiency measures the ratio of experimentally evolved gas volume to theoretically calculated gas volume. It quantifies the efficiency of electron transport in the external circuit for electrochemical reactions.

Major components of a PEM water electrolysis cell include Membrane Electrode

Assemblies (MEAs), current collectors (gas diffusion layers), and separator plates. MEAs, composed of membranes and electrocatalysts, play a crucial role in facilitating electrochemical reactions.

Noble metal-based electrocatalysts, such as Pt/Pd-based catalysts for the cathode and IrO_2/RuO_2 catalysts for the anode, are commonly used in PEM electrolysis. Efforts are underway to develop alternative electrocatalysts to reduce costs and improve efficiency.

Metal oxides, particularly IrO_2 and RuO_2, are used as electrocatalysts for OER (Oxygen Evolution Reaction). However, efforts are being made to reduce the noble metal content and improve stability by exploring mixed metal oxides and alternative catalysts.

Platinum-based catalysts are widely used for HER (Hydrogen Evolution Reaction), but research focuses on reducing Pt loading and exploring alternative catalysts such as MoS_2 and Pd-based materials to improve cost-effectiveness.

3.2.2 Alkaline Water Electrolysis

The primary elements of an Alkaline Water Electrolysis (AWE) system are the electrodes (cathode and anode), which drive the electrolysis process. The AWE system features two separate chambers: the anode and cathode compartments, divided by an ion-conductive membrane. In the anode chamber, water molecules undergo oxidation, releasing oxygen gas and creating positively charged ions (cations). Concurrently, reduction reactions in the cathode chamber convert water

molecules into hydrogen gas, generating negatively charged ions (anions). The ion-conductive membrane allows ions to pass while preventing the mixing of hydrogen and oxygen gases.

A power source connected to the electrodes supplies the electric potential necessary for electrolysis. This voltage drives ion migration toward their respective electrodes, facilitating the production of hydrogen and oxygen gases. The anode, connected to the positive terminal, attracts anions while the cathode, connected to the negative terminal, attracts cations. To maintain the electrolysis process, a continuous supply of water is directed into both chambers through inlets, where it is split into hydrogen and oxygen gases, which are then expelled through outlets.

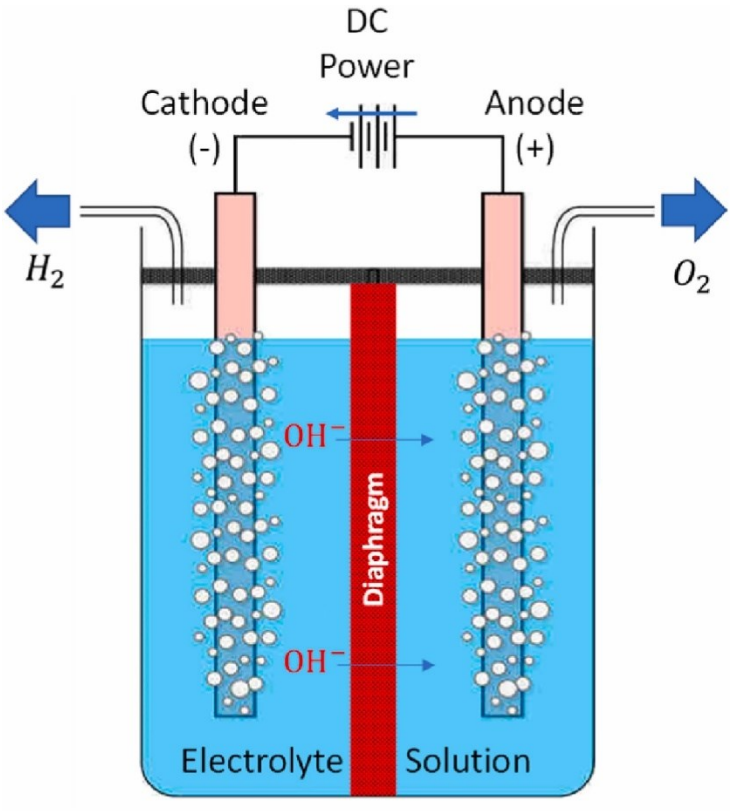

Figure 18 - Schematic of alkaline water electrolyzer.[11]

When an electric current is applied to the electrolysis cell, water molecules near the cathode undergo reduction, where hydrogen ions (H^+) gain electrons to form hydrogen gas (H_2) and hydroxide ions (OH^-). The hydroxide ions move towards the anode and undergo oxidation, releasing oxygen gas (O_2). This continuous flow of charge carriers is facilitated by the movement of hydroxide ions (OH^-) from the cathode to the anode, depending on the ionic conductivity of the electrolyte.

Electrons are transferred from the anode to the cathode through an external electric circuit, performing electrical work. AWE is a reliable and efficient

method for hydrogen production, particularly for large-scale industrial applications. The water-splitting reaction is expressed as follows:

$2H_2O(l) \rightarrow 2H_2(g) + O_2(g)$

Typically, an external Direct Current (DC) power supply is required to initiate the water-splitting process, as liquid water has poor electrical conductivity at room temperature. For AWE, the most common used electrolytes are potassium hydroxide (KOH) and sodium hydroxide (NaOH). When KOH is used, it dissociates in water into K^+ and OH^- ions, facilitating electrical conduction between the electrodes. The electrodes are typically made of conductive materials like nickel, while the ion-conductive membrane selectively allows hydroxide ions to pass through while blocking gas crossover. Once the AWE cell is powered, the following half-reactions occur:

Cathode: $2H_2O + 2e^- \rightarrow H_2 + 2OH^-$

Anode: $4OH^- \rightarrow O_2 + 2H_2O + 4e^-$

The cathodic reaction occurs at the electrode connected to the negative terminal of the DC power supply, while the anodic reaction occurs at the electrode connected to the positive terminal of the DC source. The gases collected via this

process typically exhibit high purity, around 99%, making it a very lucrative method for producing pure hydrogen.

A crucial component in this process is the separator membrane which maintains the gases within their respective compartments and acts as a safety feature to prevent combustion due to gas mixing. The AWE process is endothermic, requiring energy to carry out the reaction. The reactions produce two hydrogen molecules for every oxygen molecule. Additionally, there is no consumption of the alkaline ions (OH^-) during the process, indicating that these ions are only used to increase the conductivity of the aqueous solution and do not participate in the chemical reaction itself.

3.2.3 SOE

Solid oxide electrolysis cells (SOECs) have emerged as a pivotal technology in the field of electrochemical energy conversion, providing a sustainable solution to meet global energy demands and environmental challenges. This innovative technology stands out by using conductive ceramics instead of conventional metal-based catalysts like nickel, making it a promising approach for commercial hydrogen production.

SOECs operate at high temperatures and pressures, which enhances the thermodynamic efficiency of the water-splitting reaction. This high-temperature operation allows SOECs to achieve higher current densities and superior performance compared to other electrolysis technologies, such as alkaline

electrolysis (AE), which relies on liquid electrolytes and faces issues like electrolyte evaporation, corrosion, and contaminant build-up. SOECs eliminate these concerns and offer a more robust and efficient process.

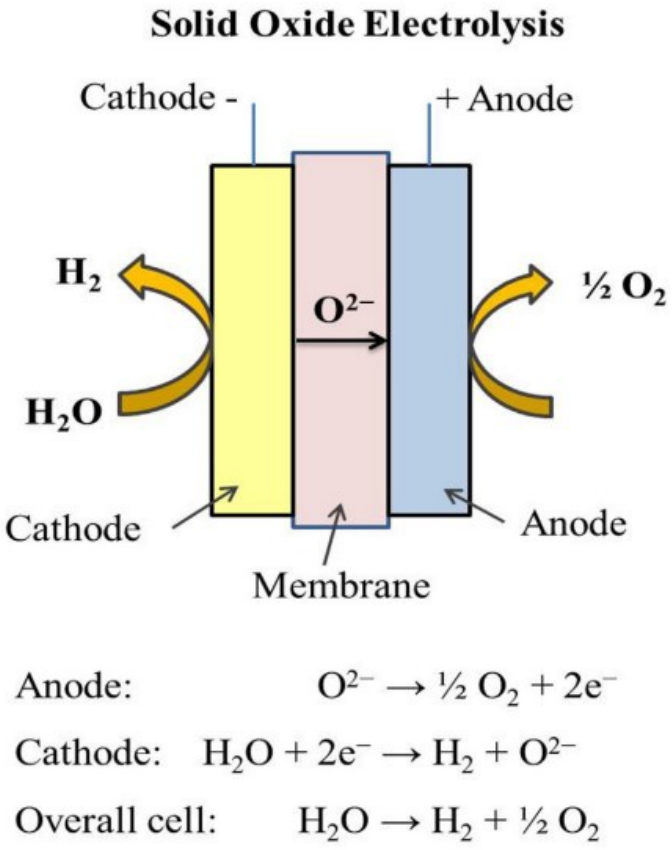

Figure 19 -Schematic illustration of Solid Oxide electrolysis.[13]

Advances in operational stability and efficiency have marked the development of SOEC water electrolysis, making it a leading technology for sustainable hydrogen production.

SOECs are also used for CO_2 electrolysis, converting carbon dioxide into valuable carbon monoxide (CO). This process targets carbon capture and utilization, although it faces challenges such as lower diffusion rates and higher activation energies compared to water electrolysis.

Via Co-Electrolysis it can be achieved to simultaneously process H_2O and CO_2, producing syngas with a tuneable H_2/CO ratio. Co-electrolysis benefits from the lower thermo-neutral voltage of water electrolysis, enhancing overall efficiency and reducing carbon deposition risks on the fuel electrode. However, achieving the desired syngas ratios can be challenging due to the reverse water gas shift reaction.

Despite their advantages, SOECs face challenges related to the cost and durability of specialized materials required for high-temperature operations. These materials have limited operational lifespans, which is a critical area for ongoing research and development.

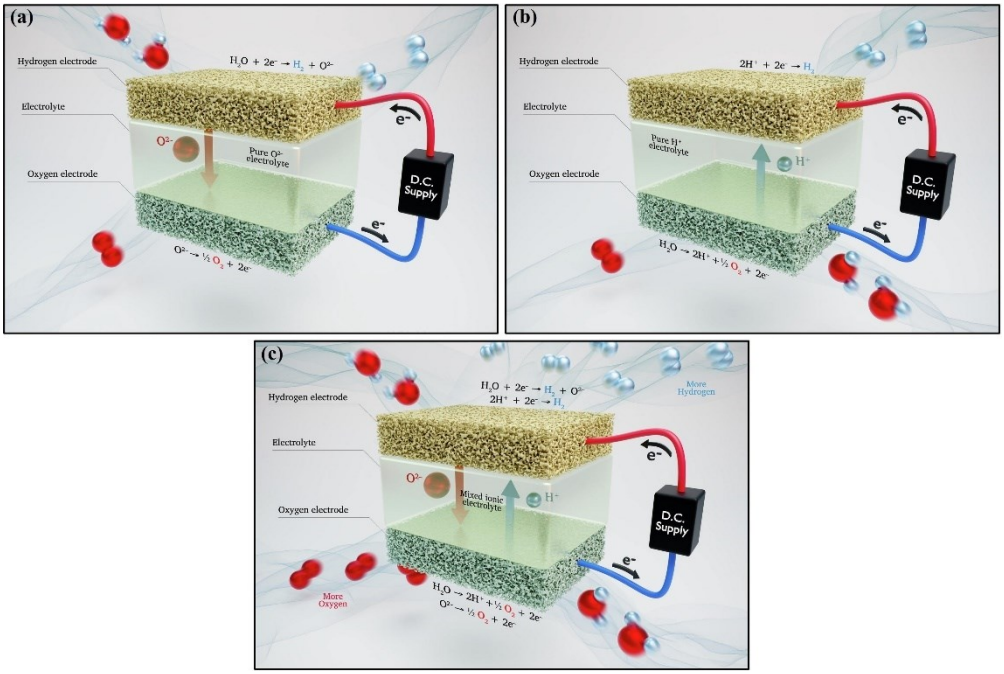

Figure 20 - 3D illustration depicting the core operating principles of (a) Oxygen-SOECs, (b) Proton-SOECs, and (c) Hybrid-SOECs.[14]

SOECs are classified into three distinct types based on their electrolyte materials: oxygen ion conducting, proton conducting, and the newly discovered Hybrid-

SOEC which simultaneously transports both oxygen ions and protons. This hybrid variant represents a significant innovation, combining the strengths of both oxygen and proton conduction.

The evolving research landscape highlights significant efforts to overcome the limitations of SOEC technology. Continued advancements in material science and operational techniques are essential for enhancing the commercial viability of SOECs. Trends in publication data underscore the growing interest and investment in this field, indicating a promising future for SOECs in the sustainable energy sector.

3.2.4 Anion Exchange Electrolysis

Anion exchange membrane (AEM) electrolysis is an emerging technology in the field of electrochemical energy conversion, garnering significant interest from academic and research institutions due to its cost-effectiveness and promising performance characteristics. Despite these advantages, the volume of research on AEM electrolysis remains relatively modest compared to traditional electrolysis methods such as Alkaline Electrolysis (AE) and Proton Exchange Membrane (PEM) electrolysis.

AEM electrolysis is notable for its potential to reduce costs associated with hydrogen production. This is primarily due to the use of less expensive materials for both the membrane and the catalysts, as opposed to the noble metals often required for PEM electrolysis.

AEM electrolysers can achieve high efficiency and current densities, making them competitive with other types of electrolysis technologies. The ability to operate under alkaline conditions reduces the risk of corrosion and allows for a broader selection of non-precious metal catalysts.

Despite its promising prospects, the academic and research community has not yet fully explored AEM electrolysis. Its cost-effectiveness and superior performance characteristics make it a compelling alternative to traditional electrolysis methods. However, to fully realize the potential of AEM electrolysers, further research is necessary to enhance energy efficiency, membrane and catalyst stability, ease of use, and overall cost-effectiveness.

3.3 Configurations of Alkaline Electrolysis Stack

Alkaline electrolysis is a widely used method for hydrogen production, particularly valuable for its low-cost and scalability. However, a single cell alkaline electrolyser generates a relatively low amount of hydrogen gas per minute, necessitating the design of electrolysis stacks to increase production.

There are two primary configurations for alkaline electrolysis cells: monopolar and bipolar. Each configuration has distinct structural and operational characteristics which influence their efficiency and application.

In a monopolar configuration, each electrolysis cell is connected in parallel to form a large module.

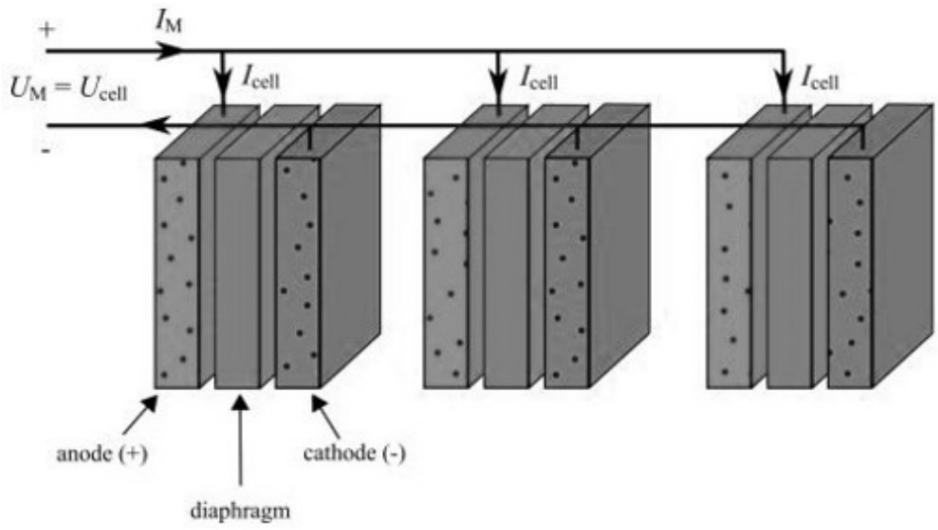

Figure 21 - Monopolar cell configuration [15]

In this setup:

- The voltage across each pair of electrodes equals the total cell voltage.
- The total current is the sum of the currents through each cell.
- The same electrochemical reaction occurs on both sides of each electrode, either hydrogen evolution or oxygen evolution, depending on the electrode polarity.

In a bipolar configuration, electrolysis cells are connected in series to form a large module.

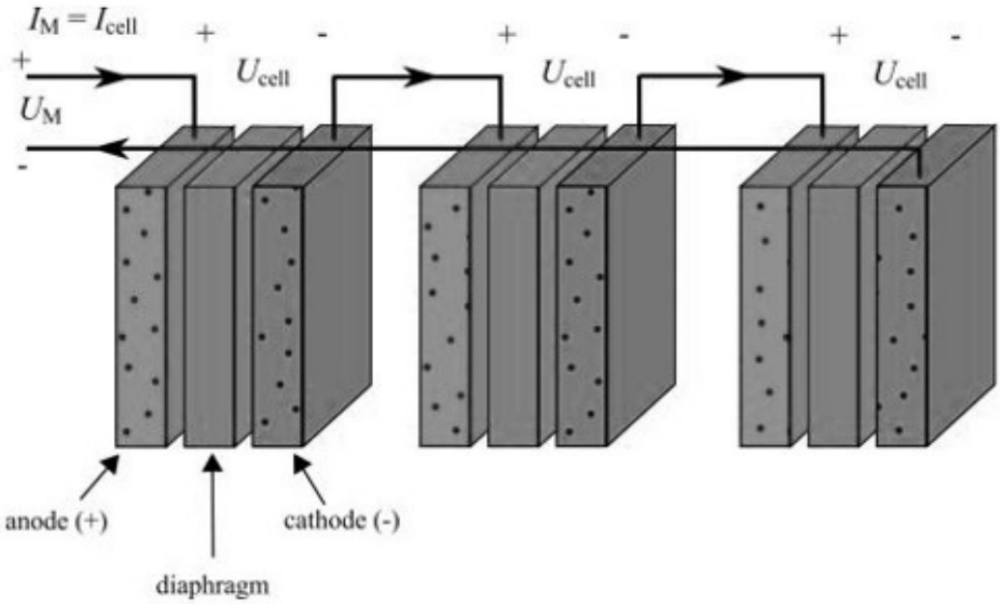

Figure 22 - Monopolar cell configuration.[15]

Key features include:

- The total voltage is the sum of voltages across each cell.
- The current passing through each cell is the same and equals the total cell current.
- Different electrochemical reactions occur on each side of the electrodes: one side acts as a cathode (hydrogen evolution) and the other as an anode (oxygen evolution).

Bipolar configurations exhibit lower ohmic losses compared to monopolar setups due to smaller gaps between electrodes, which reduces ionic transport resistance. However, these gaps must be optimally maintained to prevent electrical sparks and potential hazards.

Monopolar Stacks are easier to design and assemble, with parallel connections allowing for high current but lower voltage requirements. Ideal for systems where simplicity and ease of maintenance are prioritized.

On the other hand, bipolar stacks are more complex but offer lower ohmic losses and higher efficiency due to series connections that reduce ionic resistance. Suitable for applications requiring higher voltage and improved efficiency.

The choice between them depends on the desired balance between simplicity, efficiency, and operational requirements. Advancements in design and material selection continue to improve the performance and commercial viability of these systems, contributing to the broader adoption of hydrogen as a clean energy source.

CHAPTER 4 - MODELING OF ALKALINE ELECTROLYSERS

The number of models for electrolysis is extensive, reflecting the diversity of electrolysis technologies, the complexity of the processes involved, and the various applications and conditions under which electrolysis is performed. However, these models can be classified in some primary types of models: Empirical models, Theoretical models (e.g., thermodynamic, kinetic, transport), Mechanistic models (e.g., Butler-Volner, Nernst, Ohmic model), and specific electrolysis models (e.g., AE, AEM, SOE, PEM). Some common examples of electrolysis models include Ulleberg's and Newman's Models and Gibbs' Energy Model. Ulleberg Model is a semi-empirical model often used for hydrogen production systems. These models combine empirical data with theoretical principles to provide a more accurate and realistic representation of the electrolysis process.

Newman's Model is a mechanistic model that includes detailed descriptions of transport phenomena and electrochemical kinetics, while Gibbs' Energy Model is used for thermodynamic calculations related to the electrolysis process.

The choice of the model depends on the specific objectives of the analysis, the level of detail required, and the available data. Each type of model has its strengths and limitations, and, in practice, a combination of models may be used to gain a comprehensive understanding of the electrolysis process and optimize its performance.

4.1 Semi-Empirical Model

Several semi-empirical equations for modelling the current-voltage curve of alkaline electrolysers have been developed, with one of the most widely used models first described by Ulleberg. This model integrates thermodynamic principles, reaction kinetics, and resistive effects of the electrolyser. The fundamental expression for the current-voltage curve is provided in the equation below:

$$\boldsymbol{V_{cell} = V_{rev} + \eta_{ohm} + \eta_{act,a} + \eta_{act,c}} \qquad \textit{(6)}$$

where

V_{rev} (V) is the reversible voltage

η_{ohm} (V) is the ohmic overvoltage

$\eta_{act,a}$ (V) and $\eta_{act,c}$ (V) are, respectively, the activation overvoltage at the anode and the cathode

The above equations might be written also as:

$$\boldsymbol{V_{cell} = V_{rev} + r \cdot \left(\frac{i_{el}}{A_{elec}}\right) + s \cdot log\left[t \cdot \left(\frac{i_{el}}{A_{elec}}\right) + 1\right]} \qquad \textit{(7)}$$

Where:

V_{rev} (V) is the reversible voltage,

$r \cdot \left(\frac{i_{el}}{A_{elec}}\right)$ represents the ohmic overvoltage defined by its parameter r (Ω m^2),

the last term represents the activation overvoltage defined by the parameters *s*

(V) and t (m^2A^{-1}),

i_{el} (A) is the current absorbed by the electrolyzer,

A_{elec} (m^2) is the cell electrode active area.

The term i_{el}/A_{elec} is often referred to as the current density that can be replaced by J (A m^{-2}).

The performance of an alkaline electrolyzer is significantly influenced by its operating temperature. To enhance the aforementioned semi-empirical model, it is essential to account for the temperature effect. In this context, only the parameters r and t are temperature-dependent, while the parameter s is typically assumed to be constant. By considering the operating temperature of the electrolyzer, Ulleberg's model in Equation (7) can be revised as shown in Equation (8):

$$\boldsymbol{V_{cell} = V_{rev} + (r_1 + r_2 \cdot \theta) \cdot J + s \cdot log\left[\left(t_1 + \frac{t_2}{\theta} + \frac{3}{\theta^2}\right) \cdot J + 1\right]} \quad \textbf{(8)}$$

Where:

θ (°C) is the operating temperature,

r_1 (Ω m^2) and r_2 (Ω m^2 $°C^{-1}$) reflect ohmic losses,

t_1 (m^2 A^{-1}), t_2 (m^2 A^{-1} °C) and t_3 (m^2 A^{-1} $°C^2$) are related to the activation overvoltages and J (A m^{-2}) is the current density.

Gas pressure also affects the performance of the alkaline electrolyzer. Equation

(9) introduces new empirical parameters δ_1 (Ω m²) and δ_2 (Ω m² bar⁻¹), which account for the linear change in the ohmic overvoltage. By including the gas pressure (bar), Ulleberg's equation can be modified as follows:

$$V_{cell} = V_{rev} + \left((r_1 + \delta 1) + r_2 \cdot \theta + \delta_2 \cdot p\right) \cdot J + s \cdot log\left[\left(t_1 + \frac{t_2}{\theta} + \frac{3}{\theta^2}\right) \cdot J + 1\right] \quad (9)$$

Table 6 - Coefficients used in Ulleberg model for modelling the polarization curve.

Coefficient	Value	Unit
r_1	3.53855×10^{-4}	Ω m²
r_2	-3.02150×10^{-6}	Ω m² °C⁻¹
s	2.2396×10^{-1}	V
t_1	5.13093	m² A⁻¹
t_2	-2.40447×10^{2}	m² °C A⁻¹
t3	5.99576 × 103	m2 °C2 A⁻¹
δ1	−3.12996 × 10−6	Ω m²
δ2	4.47137 × 10−7	Ω m² bar⁻¹
p1	3.410251 × 10−4	Ω m²
p2	−7.489577 × 10−5	Ω m² mol⁻¹ L
p3	3.916035 × 10−6	Ω m² mol⁻² L²
q1	−1.576117 × 10−4	Ω m²
q2	1.576117 × 10−5	Ω m² mm⁻¹

4.1.1 Characteristic curves of the semi-empirical model

The distance between the electrode and the diaphragm (d) significantly impacts ohmic losses, which must be accounted for when formulating the I–U curve, especially at high current densities. This is because the resistance due to the distance between electrodes combines with the resistance of hydrogen and

oxygen bubbles. Thus, electrode distance is closely linked to the fluid dynamics of biphasic mixtures within the cell.

It has been demonstrated that, at a fixed electric current, the cell voltage increases linearly with the distance between electrodes, with this increment becoming more pronounced as the operating current rises. An optimal value of it can be determined using Nagai's equation:

$$\boldsymbol{d_{opt,e-e} = 1.271\ \frac{R\cdot(T+273.15)\cdot H}{F\cdot P\cdot u}\cdot i} \qquad \textit{(10)}$$

Where:

R (8.314J/(mol) is the universal gas constant,

T (°C) is the temperature,

H (m) is the height of the electrode,

F is the Faraday's constant, approximately 96485 C/mol,

P (atm) is the pressure in the system,

u (m/s) is the rising velocity of bubbles,

i is the current in amperes (A).

When the distance exceeds this optimal value, its reduction decreases the voltage. However, once the optimum distance is reached, further reduction increases the

voltage. This phenomenon occurs because, at very low electrode-diaphragm distances, the bubble fraction becomes so high that the electrolyte resistance increases significantly, thus raising the required voltage for electrolysis.

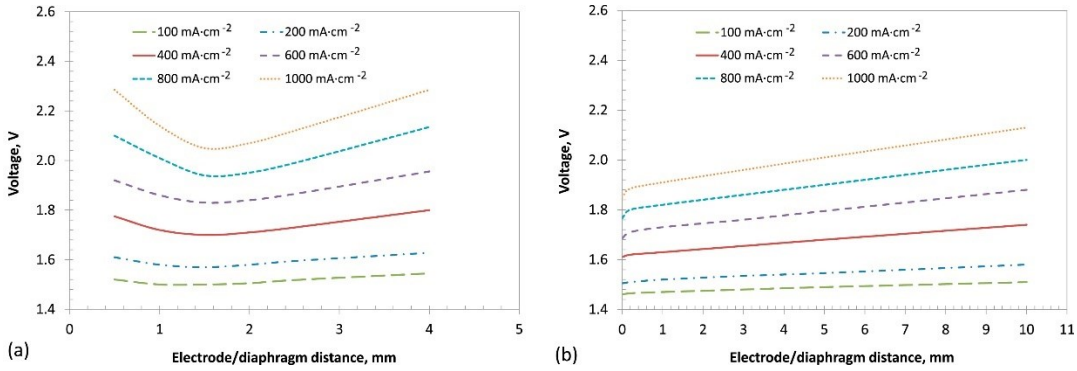

Figure 23 - Cell voltage as a function of the distance between electrode and diaphragm (10 M KOH, 100 °C, ambient pressure): (a) sheet electrodes; (b) porous electrodes [16]

The distance between electrodes in electrochemical cells affects gas bubble velocity (u): faster gas removal reduces bubbles, shortening the optimal distance (d_{opt}) and lowering electrolyte resistance. Higher forced convection enhances water electrolysis efficiency. However, higher current density increases gas generation, penetrating the medium and reducing conductivity. At very high current densities or low electrolyte velocities, conductivity drops as gas fills the space between electrodes.

For porous electrodes or d > $d_{opt,e\text{-}d}$ in sheet electrodes, ohmic resistance (q) decreases linearly with electrode/diaphragm distance (Equation 9):

$$\boldsymbol{q = q_1 + q_2 \cdot d} \qquad \textbf{(11)}$$

Here, q_1 (Ω m^2) and q_2 (Ω m^2 mm^{-1}) represent ohmic losses.

This equation doesn't apply for $d < d_{opt,e\text{-}d}$ in porous electrodes, where the trend reverses.

In alkaline water electrolysis, the conductivity of the electrolyte, typically KOH or NaOH solutions, is crucially influenced by the movement and concentration of OH^- ions. Various studies have explored how electrolyte conductivity (k) varies with concentration (C) and operating temperature (T).

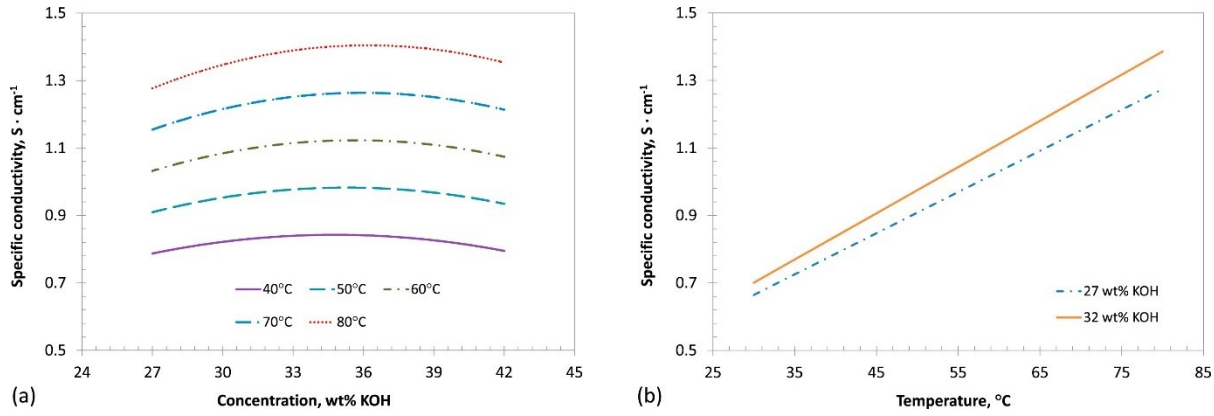

Figure 24 -Specific conductivity obtained experimentally: (a) specific conductivity vs. KOH concentration at 40, 50, 60, 70 and 80 °C; (b) specific conductivity vs. temperature at 22, 27 and 32 wt% KOH.[16]

Typically, within the temperature range of 60–80 °C, peak conductivity is found around 34–38%wt KOH. Additionally, it can be observed a quadratic relationship between conductivity and concentration at a given temperature within this range. There's a linear increase in specific conductivity with temperature at a constant KOH concentration typical for operating conditions.

A polarization curve is a graph that illustrates the relationship between the voltage applied to the electrolyzer and the resulting current density during electrolysis. This curve is fundamental for evaluating the efficiency and performance of electrolyzers and can be generated by incrementing the current, with additional data points collected in the initial nonlinear region to capture activation overpotentials along with parameters such as cell voltage, current, hydrogen production rate, and temperatures of the electrolyte, hydrogen outlet, and separators.

In summary, the influence of operating temperature, electrolyte concentration, and electrode/diaphragm distance on alkaline electrolyzers is significant and well-documented.

Increasing temperature decreases the voltage required for electrolysis within the range of 20–80 °C. This effect is attributed to lower reversible voltages and improved reaction kinetics.

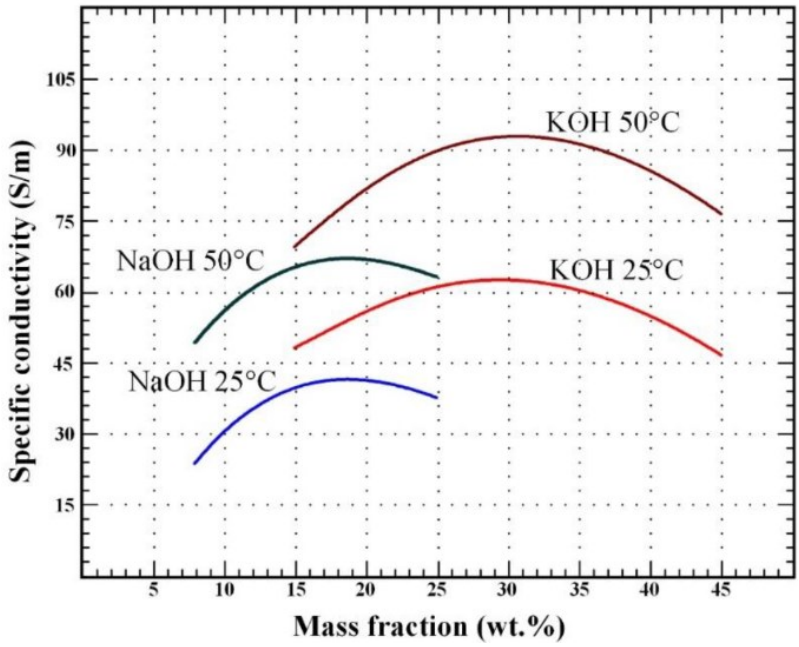

Figure 25 -Specific electrolyte conductivity for liquid solutions based on either KOH or NaOH according to the mass fraction of the solution.[17]

Optimal performance occurs around 34–38 wt% KOH and 15-22% wt% NaOH, where energy consumption is minimized due to enhanced electrolyte conductivity. Below this range, conductivity is insufficient, while above it, ion concentration limits species transfer.

The distance between electrodes significantly affects ohmic overpotentials in alkaline electrolysis. Decreasing this distance typically enhances overall conductivity, but excessive reduction can lead to increased void fraction and reduced conductivity. The optimal distance varies with bubble rising velocity and current density, impacting electrolyzer efficiency as shown in experimental validations.

Overall, these factors are critical in optimizing the performance of alkaline

electrolyzers, influencing their energy efficiency and operational stability under varying conditions of temperature, electrolyte concentration, and electrode configuration.

4.2 Empirical Model

The voltage of the cell, including the different voltages is given by:

$$V_{cell} = V_{rev} + (R_a + R_c + R_{ele} + R_{mem}) \cdot i_{el} + \eta_{act,a} + \eta_{act,c} \qquad (12)$$

Where:

V_{rev} (V) is the reversible voltage,

R_a (Ω) and R_c (Ω) are the ohmic resistances related to the conductivity of the electrodes (anode and cathode), respectively,

R_{ele} (Ω) represents the ohmic loss due to the electrolyte conductivity,

R_{mem} (Ω) stands for the membrane ohmic resistance,

$\eta_{act,a}$ (V) and $\eta_{act,c}$ (V) are the activation overvoltage at the anode and the cathode respectively.

The reversible potential is defined as the voltage required to initiate the electrolysis reaction. Its value is directly related to the Gibbs energy:

$$\Delta G = \Delta H - T \cdot \Delta S \qquad (13)$$

Where:

ΔH (J/mol) is the change in enthalpy,

ΔS (J/mol∗K) is the change in entropy,

and T (K) is the temperature.

The reversible potential V_{rev} is the ratio of the Gibbs energy ΔG to the product of Faraday's constant F and the number of exchanged electrons n, as given below:

$$\mathbf{V_{rev}=\Delta G/(n\cdot F)} \qquad \mathbf{(14)}$$

The change in enthalpy ΔH is also related to the thermoneutral cell voltage V_{th} by the following equation:

$$\boldsymbol{V_{th}=\Delta H/(n\cdot F)} \qquad \boldsymbol{(15)}$$

Given that the number of electrons n=2 and the Faraday's constant is F=96485 C/mol, at standard conditions (T=298.15, pressure of 1 bar), the values of the enthalpy ΔH and the entropy ΔS are given as: ΔH=285.84 kJ/mol, ΔS=0.1631kJ/mol*K. At these conditions, the reversible potential and the thermoneutral cell voltage are, respectively, given by: $V_{rev,0}$=1.23V and $V_{th,0}$=1.48V. At other operating conditions, the reversible potential V_{rev} (V) is determined using Nernst's equation.

The activation overvoltages starting the water electrolysis process at the anode $\eta_{act,a}$ and at the cathode $\eta_{act,c}$ can be evaluated using the Butler–Volmer equations (or Tafel's approximations):

$$\eta_{act,a} = \frac{2.3 \cdot R \cdot T}{\alpha_a \cdot F} \cdot log\left(\frac{j_a}{j_{0,a}}\right) \qquad (16)$$

$$\eta_{act,c} = \frac{2.3 \cdot R \cdot T}{\alpha_c \cdot F} \cdot log\left(\frac{j_c}{j_{0,c}}\right) \qquad (17)$$

where:

α_a and α_c are the charge transfer coefficients at the anode and the cathode, respectively.

j_a (mA/cm^2) and j_c (mA/cm^2) are the current densities at the anode and the cathode, respectively.

$j_{0,a}$ (mA/cm^2) and $j_{0,c}$ (mA/cm^2) are the exchange current densities at the anode and the cathode, respectively

Alkaline electrolyzers are composed of various elements, each modelled as electrical resistance. The total ohmic resistance of the electrolyzer can be expressed as:

$$R_{total} = R_a + R_c + R_{ele} + R_{mem} \qquad (18)$$

Where:

R_a (Ω) and R_c (Ω) are the anode and cathode resistances,

R_{ele} (Ω) the resistance of the electrolyte (KOH or NaOH),

and R_{mem} the resistance of the membrane.

In an alkaline electrolyzer, the electrodes can be made of cobalt, nickel, or iron. Nickel is the preferred material for most electrodes due to its stability. The resistances of the anode and cathode are influenced by the electrodes' conductivity and geometry.

During alkaline electrolysis, the electrolyte's resistance R_{ele} consists of bubble-free resistance and bubble-induced resistance.

In summary, the empirical model of alkaline electrolyzers details the resistances and conductivities of electrodes, electrolytes, and membranes, considering temperature and material properties.

4.3 Alkaline electrolyzer in DIISM

An alkaline electrolyzer has been installed at the Department of Industrial Engineering and Mathematical Sciences (DIISM) of the Polytechnic University of Marche. Installed by Erre Due S.p.A., the specific model chosen is the Mercury Expert G6 electrolyser. The Mercury series is renowned for its robustness and reliability, requiring minimal maintenance while offering advanced remote monitoring capabilities. This ensures operational stability and the ability to

troubleshoot in real time from anywhere in the world via internet connection.

Figure 26 – Alkaline electrolyzer installed at DIISM [18]

The system operates by electrolytically dissociating water molecules into hydrogen and oxygen gases, which are then separated by specialized membranes and collected at pressures up to 30 bar through a dedicated booster. The gases undergo further purification and drying processes as needed to meet specific purity standards.

Hydrogen generated by such systems finds diverse applications across industries, including electronics, transport fuels, and clean energy storage solutions. The Mercury Expert G6 is versatile, catering to a wide range of operational needs from simple applications to more complex requirements such as those in nuclear power generation.

Moreover, Erre Due offers an integrated "D" version of the Mercury generators, incorporating a purifier which enhances economic efficiency, reduces installation time, and optimizes space utilization. This feature is particularly beneficial in

applications requiring high gas purity levels, such as welding and heat treatments. DIISM owns a Mercury Expert G6 electrolyser. Its technical specifications are reported below:

Table 7 - Technical specifications of Mercury Expert G6 [18]

Feature	Unit	Value
Dimensions	mm	850x1350x1870
Weight	kg	300
Hydrogen production	mc/h	4
Oxygen production	mc/h	2
Hydrogen and oxygen pressure	bar	5
Hydrogen purity	%	99,5%
Oxygen purity	%	99%
Dew Point (model D)	%	saturated
Power supply		3x400Vac - 50Hz
Power consumption	kWh	22.3

CHAPTER 5 - ELECTROLYZER DESIGN USING ASPEN PLUS

5.1 Introduction to Aspen HYSYS Software

Aspen Plus is a leading process simulation software widely used in the chemical engineering and energy sectors for designing, modelling, and optimizing various processes. This powerful tool allows to create detailed simulations of complex systems, providing insights into performance, efficiency, and cost-effectiveness. In the context of hydrogen production, Aspen Plus serves as an invaluable resource for developing and refining technologies such as alkaline water electrolysis.

In this study, Aspen Plus is used to develop a model of an alkaline water electrolysis system. This model includes the electrochemical behaviour of the cell stack and the various interactions between components. By simulating these elements, we can predict the performance of the system under different conditions, identify potential improvements, and ensure efficient and reliable hydrogen production.

The flexibility of Aspen Plus in handling complex simulations, coupled with its ability to integrate custom subroutines, makes it an ideal tool for advancing the technology of hydrogen production.

5.2 System configuration

Figure 26 shows the schematic diagram of the Alkaline Water Electrolysis (AWE) system, comprising an electrolysis stack, heater, pumps, and phase separators. The AWE stack is modelled using an RStoic reactor block to handle the electrochemical reactions.

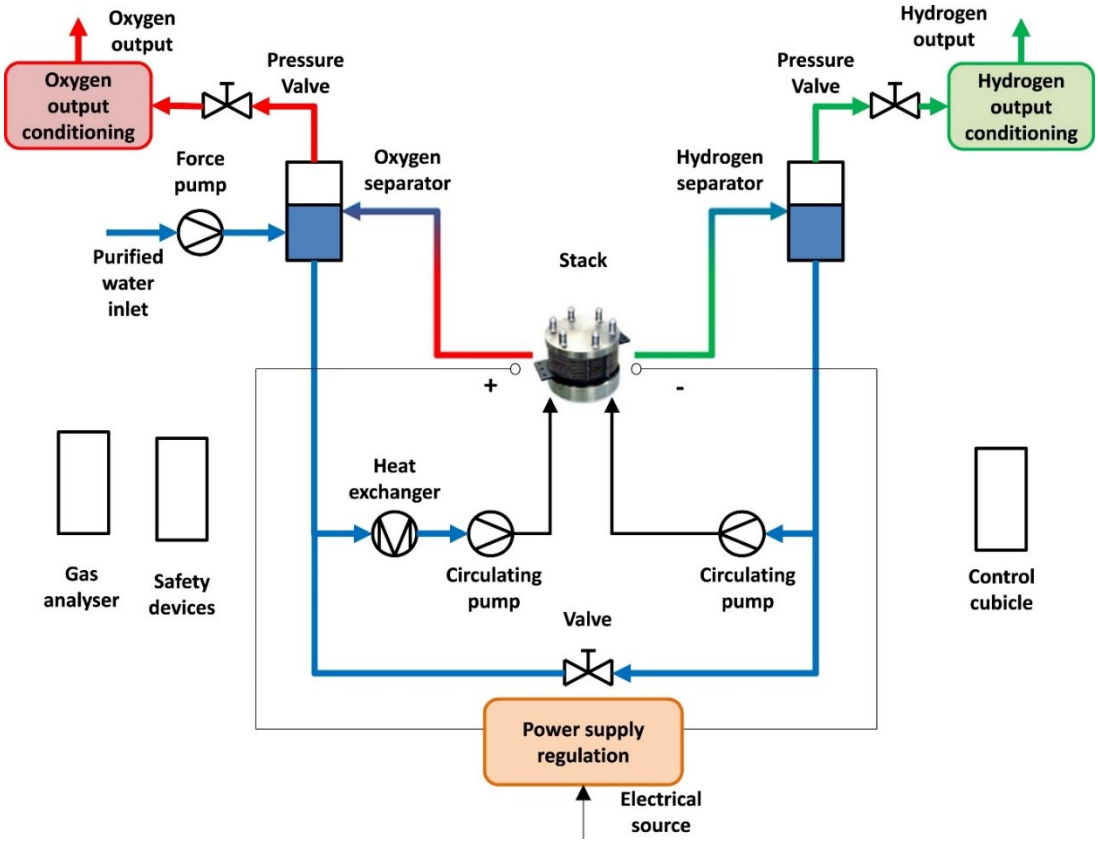

Figure 27 - Schematic diagram of the AWE system[19]

Hydrogen and oxygen are initially generated as gases dissolved in the liquid electrolyte. Once saturation is reached, excess gas forms bubbles. During operation, the exhaust flow from both the anode and cathode contains these gas

bubbles and liquid. To achieve high-purity hydrogen and oxygen, the gases pass through phase separators and condensers, which remove water.

The electrolyte from the phase separator is recirculated to the stack by pumps.

5.3 Main components of the model

5.3.1 Electrolyzer Stack

Electrolyzer Stack is the core of the AWE system where the electrolysis reaction takes place. Water is split into hydrogen and oxygen using an electrical current. It consists of a RStoic reactor and a separator.

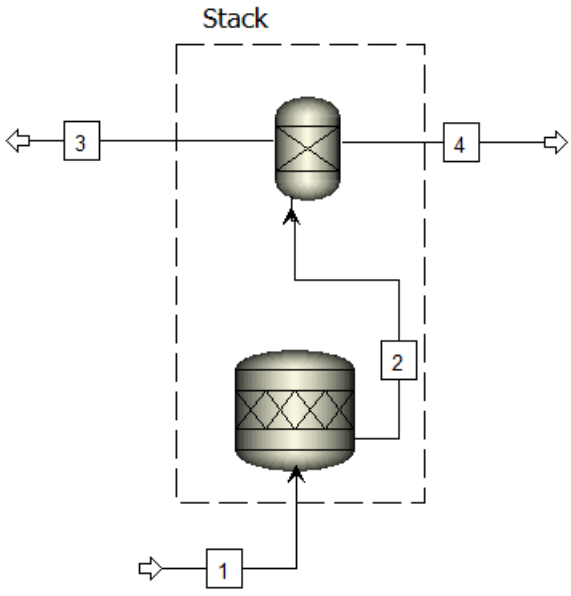

Figure 28 – Electrolyzer stack.

RStoic Reactor is a type of reactor model in Aspen Plus used to simulate chemical reactions where stoichiometry of the reaction is known. It is suitable for scenarios where precise kinetic data is not required, making it ideal for electrolysis

processes in the AWE system where the focus is on the overall reaction rather than the detailed kinetics.

After the electrolysis reaction in the stack (RStoic reactor), the mixed stream containing hydrogen, oxygen, and the electrolyte enters a separator block. The Separator Block is a critical component in the AWE system, playing a key role in managing the separation of gases and liquids post-electrolysis. It separates the hydrogen and oxygen gases from the liquid electrolyte by specifying splits for each component in each substream.

This separation ensures that the gas phase (hydrogen and oxygen) is properly isolated from the liquid phase (electrolyte). This allows precise control over the purity and flow rates of the separated streams. Most of the hydrogen and oxygen gases would be directed to their respective gas separators (H2-SEP and O2-SEP), while the liquid electrolyte is recirculated back into the system.

5.3.2 Hydrogen separator block

The H2-SEP block is designed to further purify hydrogen gas that has already been initially separated from the electrolyte mixture by the preceding separator block. This ensures that the hydrogen gas output is of high purity.

As input is takes the stream that carries hydrogen gas that has been separated from the electrolyte by the previous separator block part of the electrolyzer stack. This stream primarily consists of hydrogen gas with minimal liquid electrolyte content.

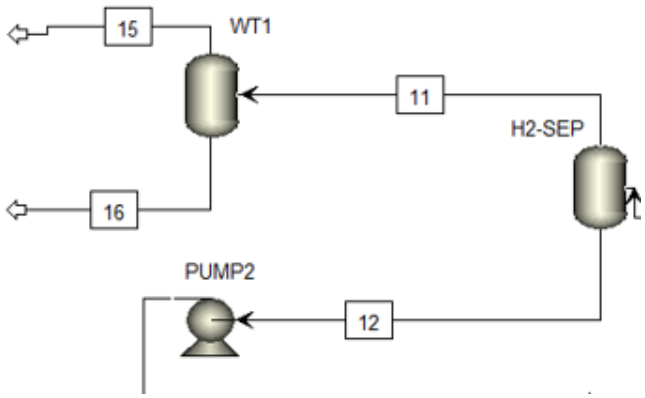

Figure 29 - Hydrogen separator block.

The H2-SEP block performs an additional separation to ensure that any remaining electrolyte or impurities are removed from the hydrogen gas. This can involve techniques such as condensation or scrubbing to purify the hydrogen ensuring that most of the hydrogen is directed to the output stream while any residual liquid or impurities are removed.

The stream carrying any remaining electrolyte and impurities that were separated from the hydrogen gas is typically recirculated back into the system and maintain system efficiency.

5.3.3 Oxygen separator block

The O2-SEP block is designed to further purify oxygen gas that has already been initially separated from the electrolyte mixture by the preceding separator block. This ensures that the oxygen gas output is of high purity.

The input stream to the O2-SEP block carries oxygen gas with minimal liquid electrolyte content that has been separated from the electrolyte by the previous

separator block.

Within the O2-SEP block, the component splits are set to maximize the purity of the oxygen gas. This ensures that most of the oxygen is directed to the output stream while any residual liquid or impurities are removed. The stream carrying any remaining electrolyte and impurities that were separated from the oxygen gas is typically recirculated back into the system.

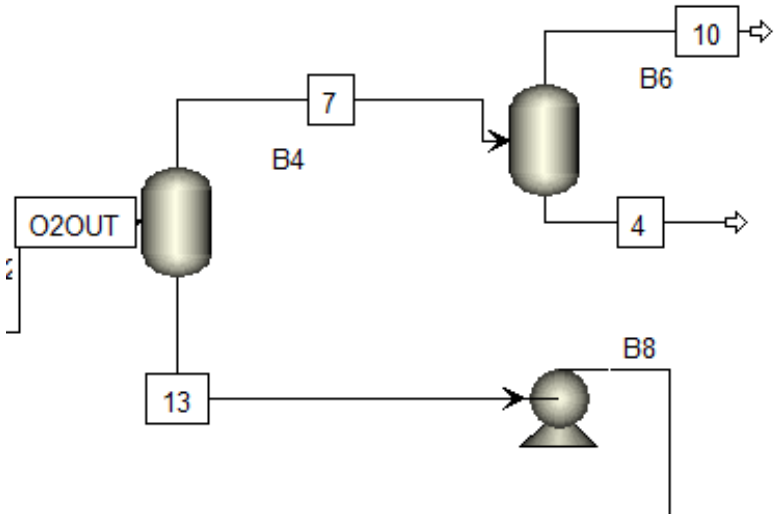

Figure 30 - O2 separator block.

The O2-SEP block is a crucial component in the AWE system for achieving the highest possible purity of oxygen gas. It takes oxygen that has been initially separated by the preceding separator and removes any remaining impurities or liquid electrolyte. By effectively segregating oxygen, the O2-SEP ensures that the output oxygen stream meets the required purity standards for its intended applications.

5.3.4 Impurity handling block

The output streams from the previous H2-SEP and O2-SEP blocks, which carry any remaining electrolyte and impurities separated from the hydrogen and oxygen gases, respectively, are directed to a mixer block. Mixer combines streams into one outlet stream. The combined stream of impurities from the mixer block is then passed through a Heat Exchanger (HE). The primary purpose of the heat exchanger is to either cool or heat the combined stream to the desired temperature before it is re-fed into the electrolysis system.

The heat exchanger adjusts the temperature of the stream to ensure optimal conditions for the electrolyte when it is returned to the system.

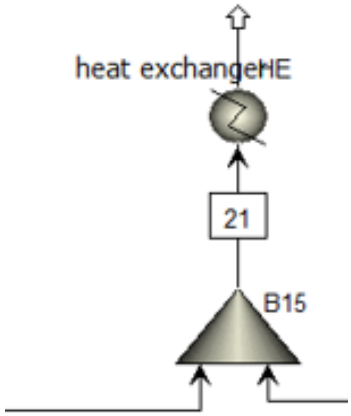

Figure 31 - Impurity handling block.

This recirculated stream helps maintain system efficiency and balance by ensuring that the electrolyte and any remaining impurities are continually

processed.

5.4 Simulation tuning

The Aspen simulation was tuned using measured data directly obtained from the electrolyser installed at DIISM (Department of Industrial Engineering and Mathematical Sciences) of the Polytechnic University of Marche. This process ensures that the simulation accurately reflects the real-world performance and operational characteristics of the electrolyser system. By integrating empirical data into the Aspen model, the theoretical value of hydrogen production rates, energy consumption, and system efficiencies have been calculated. This approach not only validates the reliability of the simulation, but also enhances its utility in guiding future design improvements and operational strategies for hydrogen generation and utilization systems.

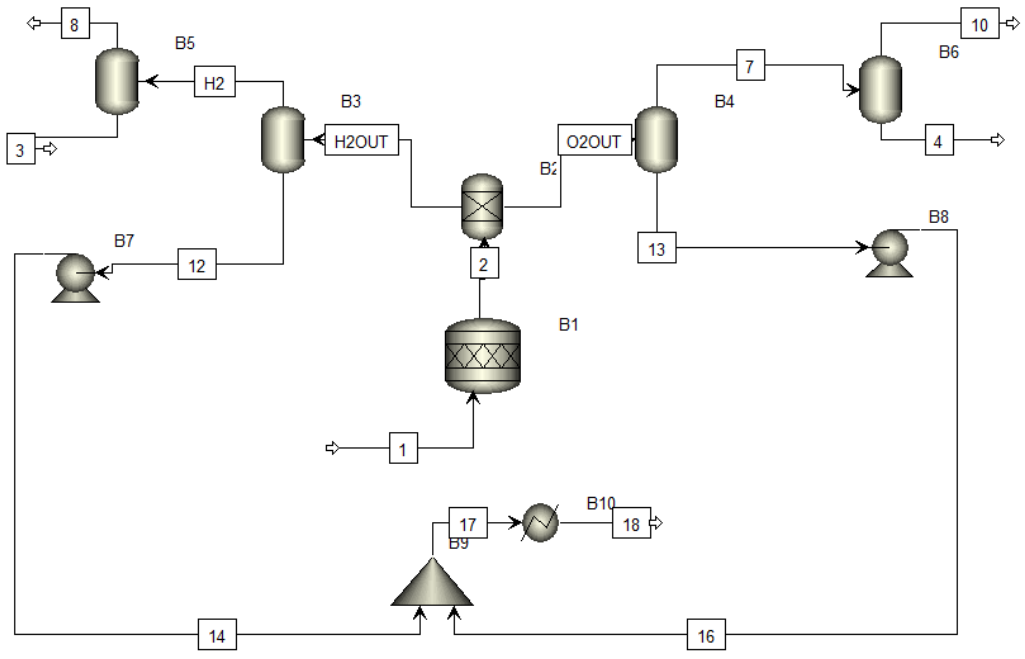

Figure 32 –Aspen Plus Simulation.

5.4.1 Experimental data

Experiments were conducted across a range of temperatures (25°C, 30°C, 35°C, and 40°C) at pressure 4.5 bar using an electrolyte solution consisting of 18% NaOH. The electrolyser system under investigation featured an active cell area of 450 cm^2 spread across 160 individual cells. During these experiments, several parameters were measured and recorded. These parameters included Current Density (A/cm^2), which indicates the rate of current passing through the electrolyser per unit area; Cell Voltage (V), which denotes the electrical potential difference across the electrolysis cell; Hydrogen Flow Rate (Nm^3/h), indicating the volume of hydrogen gas produced per hour; and Oxygen Flow Rate (Nm^3/h), representing the volume of oxygen gas generated over the same period.

5.4.2 Aspen Plus simulation input data

In the Aspen simulation, the input power was calculated using data derived from measured parameters. Specifically, the cell voltage (V_{cell}), number of cells (N), active area (A_{elec}), and current density (J) obtained from experimental measurements were all integrated into the simulation model.

Input power of the RStoich reactor was calculated as:

$$\boldsymbol{P = V_{cell} \cdot N \cdot A_{elec} \cdot J} \quad \textbf{(19)}$$

The data that were received at each temperature are reported on the table below:

Table 8 - Input Power for the RStoich reactor

Temperature (°C)	Pressure (bar)	Current Density (A/cm2)	Cell Voltage (V)	Power (Watt)
25.00	4.50	0.05	2.04	7172.00
25.00	4.50	0.05	2.06	7920.00
25.00	4.50	0.07	2.10	10080.00
25.00	4.50	0.08	2.15	12384.00
25.00	4.50	0.07	2.11	11121.00
25.00	4.50	0.06	2.08	8964.00
30.00	4.50	0.06	2.05	8856.00
30.00	4.50	0.04	1.98	6004.00
30.00	4.50	0.06	2.05	9184.00
30.00	4.50	0.06	2.07	9599.00
30.00	4.50	0.08	2.12	12882.00
30.00	4.50	0.08	2.10	12432.00
35.00	4.50	0.07	2.06	10528.00
35.00	4.50	0.07	2.04	9780.00
35.00	4.50	0.06	2.03	9072.00
35.00	4.50	0.05	1.98	7608.00
35.00	4.50	0.08	2.09	12692.00
40.00	4.50	0.09	2.07	13240.00
40.00	4.50	0.04	1.89	5436.00
40.00	4.50	0.06	1.96	8478.00
40.00	4.50	0.06	1.98	9164.00
40.00	4.50	0.06	1.95	8112.00
40.00	4.50	0.04	1.84	5015.00
40.00	4.50	0.06	1.95	8112.00
40.00	4.50	0.03	1.81	4046.00
40.00	4.50	0.05	1.91	6405.00

This method ensured that the input power accurately reflected the real-world

operational characteristics of the electrolyser system.

Additionally, the electrolyte inlet stream into the simulation was computed based on technical specifications, taking into account the concentration of NaOH at 18%.

It was calculated as:

$$\dot{m}_{inlet} = \frac{3.4}{4} \cdot \dot{m}_{H2} + \left(\frac{3.4}{4} \cdot \dot{m}_{H2}\right) \cdot \frac{[NaOH]}{[H20]} \quad (20)$$

where

3.4 and 4 represent the rated water consumption (kg/h) and rated H_2 production (Nm^3), respectively, while [NaOH] and [H_2O] represent the concentration of NaOH and H_2O in the electrolyte.

Table 9 - Input values for the electrolyte

Temperature (°C)	Pressure (bar)	H2_flow (Nm3/h)	Inlet_flow (kg/h)
25.00	4.50	1.40	1.45
25.00	4.50	1.60	1.66
25.00	4.50	1.92	1.99
25.00	4.50	2.30	2.38
25.00	4.50	2.11	2.19
25.00	4.50	1.72	1.78
30.00	4.50	1.66	1.72
30.00	4.50	1.21	1.25
30.00	4.50	1.79	1.86
30.00	4.50	1.85	1.92
30.00	4.50	2.43	2.52
30.00	4.50	2.36	2.45
35.00	4.50	2.04	2.11
35.00	4.50	1.85	1.92
35.00	4.50	1.72	1.78
35.00	4.50	1.47	1.52
35.00	4.50	2.49	2.58
40.00	4.50	2.62	2.72
40.00	4.50	1.21	1.25

40.00	4.50	1.72	1.78
40.00	4.50	1.85	1.92
40.00	4.50	1.66	1.72
40.00	4.50	1.02	1.06
40.00	4.50	1.72	1.78
40.00	4.50	0.89	0.92
40.00	4.50	1.40	1.45

These calculations were crucial for accurately modelling the electrolyte composition within the Aspen framework.

By incorporating these calculations into the Aspen simulation, we could effectively simulate and analyze the performance of the electrolyser system in order to do a comparison between the theoretical values and real data.

CHAPTER 6 - RESULTS

In order to assess the hydrogen and oxygen production flow rates, an Aspen Plus simulation was conducted for each of the experimental temperatures (25°C, 30°C, 35°C, and 40°C). For each temperature setting, the simulation was updated to reflect the corresponding power input and electrolyte inlet flow based on empirical data. The power input was calculated as the product of cell voltage (V_{cell}), number of cells, active cell area, and current density derived from the measured data. The inlet water stream was determined according to technical specifications, incorporating an 18% NaOH concentration. This approach ensured that the simulation accurately mirrored real-world conditions, providing reliable insights into the electrolyser's performance and the resulting hydrogen and oxygen production rates.

6.1 Hydrogen and Oxygen flow rate evaluation

After running the simulations, the hydrogen flow rates were obtained for each temperature. These simulated hydrogen flow rates were then compared with the empirically measured data to assess the accuracy and reliability of the simulation model. By evaluating the differences between the simulated and empirical data, the study aimed to quantify the error and understand the potential sources of discrepancies.

Table 10 - Empirical vs Simulation values of Hydrogen and Oxygen flow rates at operating temperature of 25°C

T (°C)	H2_em (kg/h)	O2_em (kg/h)	H2_sim (kg/h)	O2_sim (kg/h)	Error_H2 %	Error_O2 %
25	0.12	0.99	0.13	1.00	1.20	1.21
25	0.14	1.13	0.14	1.14	1.20	1.21
25	0.17	1.35	0.17	1.37	1.20	1.21
25	0.20	1.62	0.21	1.64	1.20	1.21
25	0.19	1.48	0.19	1.50	1.20	1.67
25	0.15	1.21	0.15	1.23	1.20	1.21
Avg	**0.16**	**1.30**	**0.17**	**1.31**	**1.20**	**1.28**

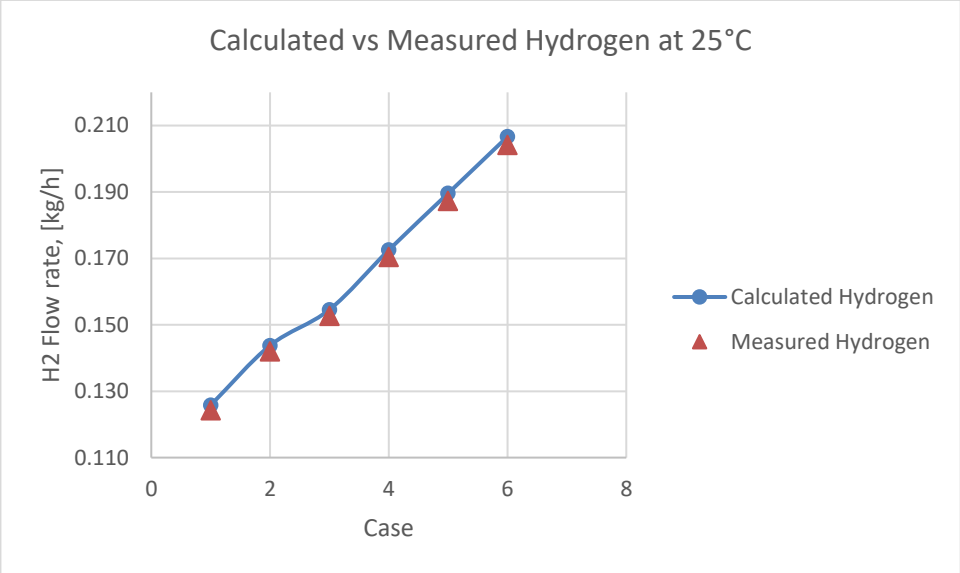

Figure 33 - Calculated vs Measured hydrogen flow rate trends at operating temperature of 25°C

Table 11 - Empirical vs Simulation values of Hydrogen and Oxygen flow rates at operating temperature of 30°C

T (°C)	H2_em (kg/h)	O2_em (kg/h)	H2_sim (kg/h)	O2_sim (kg/h)	Error_H2 %	Error_O2 %
30	0.15	1.17	0.15	1.18	1.20	1.21
30	0.11	0.85	0.11	0.86	1.20	2.02
30	0.16	1.25	0.16	1.28	1.20	1.76
30	0.16	1.30	0.17	1.32	1.20	1.74
30	0.22	1.70	0.22	1.73	1.20	1.61
30	0.21	1.66	0.21	1.68	1.20	1.21
Avg	**0.17**	**1.32**	**0.17**	**1.34**	**1.20**	**1.59**

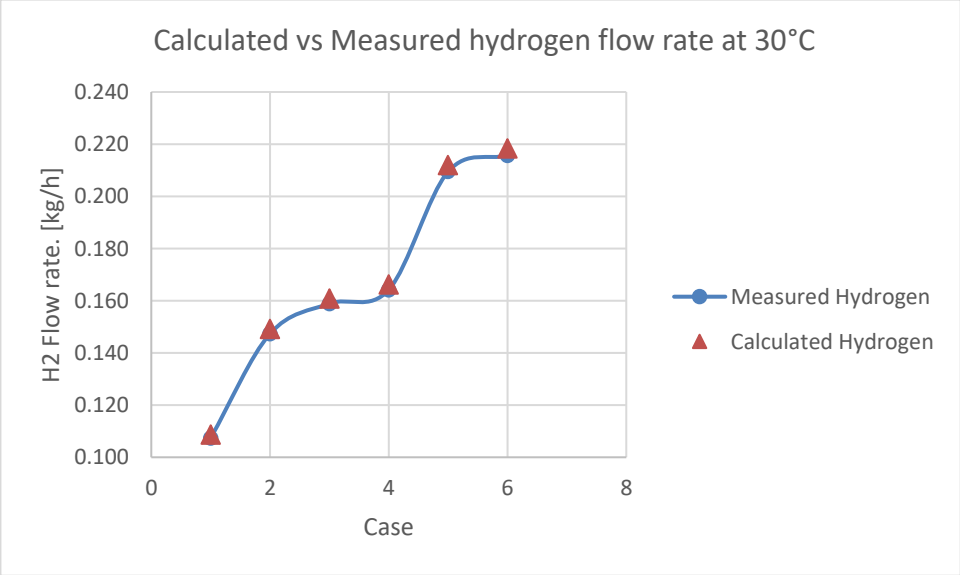

Figure 34 - Calculated vs Measured hydrogen flow rate trends at operating temperature of 30°C

Table 12 - Empirical vs Simulation values of Hydrogen and Oxygen flow rates at operating temperature of 35°C

T (°C)	H2_em (kg/h)	O2_em (kg/h)	H2_sim (kg/h)	O2_sim (kg/h)	Error_H2 %	Error_O2 %
35	0.18	1.44	0.18	1.45	1.20	1.21
35	0.16	1.30	0.17	1.32	1.20	1.74
35	0.15	1.21	0.15	1.23	1.20	1.21
35	0.13	1.03	0.13	1.05	1.20	1.88
35	0.22	1.75	0.22	1.78	1.20	1.60
Avg	**0.17**	**1.34**	**0.17**	**1.36**	**1.20**	**1.53**

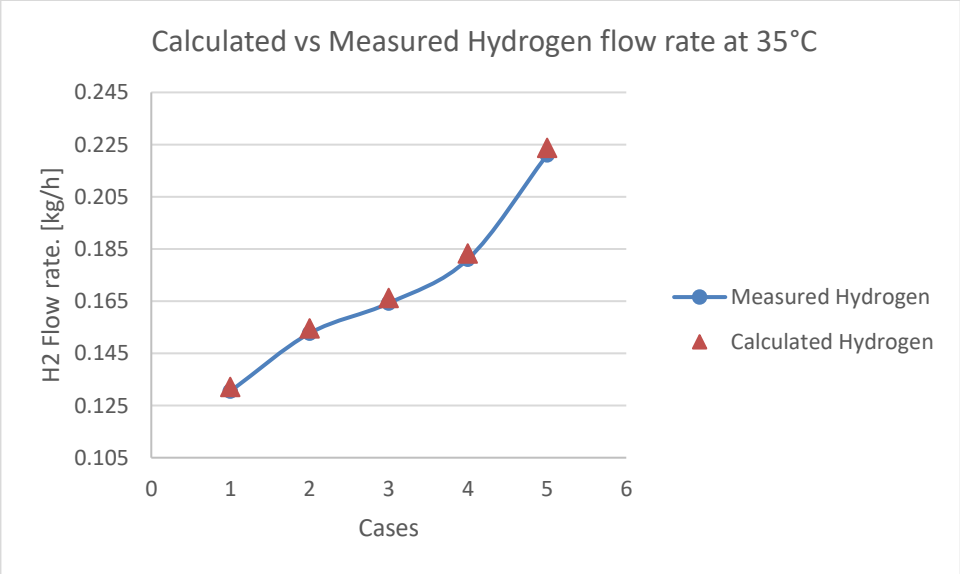

Figure 35 - Calculated vs Measured hydrogen flow rate trend at operating temperature of 35°C

Table 13 - Empirical vs Simulation values of Hydrogen and Oxygen flow rates at operating temperature of 40°C

T (°C)	H2_em (kg/h)	O2_em (kg/h)	H2_sim (kg/h)	O2_sim (kg/h)	Error_H2 %	Error_O2 %
40	0.23	1.85	0.24	1.87	1.20	1.21
40	0.11	0.85	0.11	0.86	1.20	2.02
40	0.15	1.21	0.15	1.23	1.20	1.21
40	0.16	1.30	0.17	1.32	1.20	1.74
40	0.15	1.17	0.15	1.18	1.20	1.21
40	0.09	0.72	0.09	0.73	1.20	1.21
40	0.15	1.21	0.15	1.23	1.20	1.21
40	0.08	0.62	0.08	0.63	1.20	2.32
40	0.12	0.99	0.13	1.00	1.20	1.21
Avg	**0.14**	**1.10**	**0.14**	**1.12**	**1.20**	**1.48**

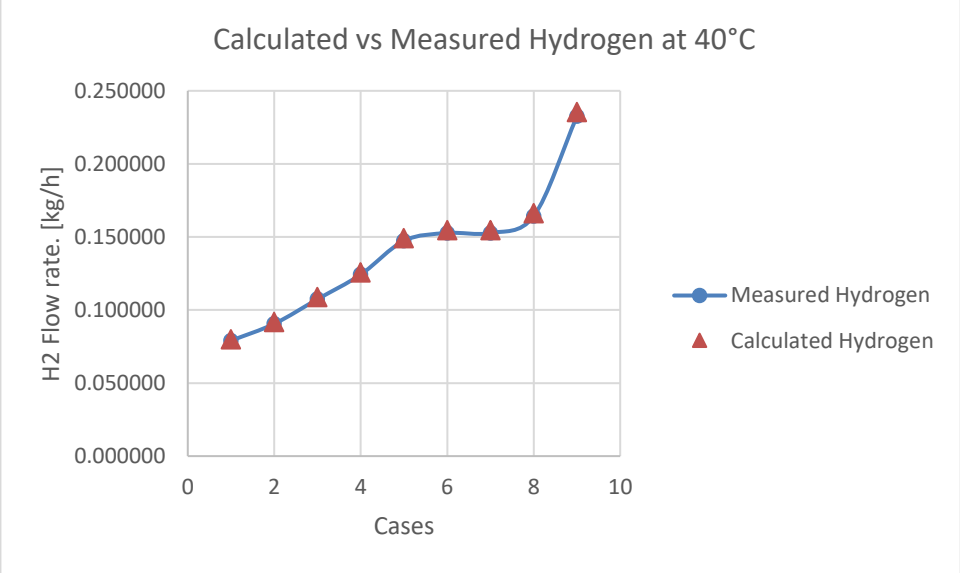

Figure 36 - Calculated and Measured hydrogen flow rate trend at operating temperature of 40°C

This comparison provided useful insights into the performance of the

electrolyser. Below there is a graphical presentation of the error between the theoretical values obtained from Aspen Simulation and the measured values. In all cases the theoretical values are between 1-2% higher than the measured values.

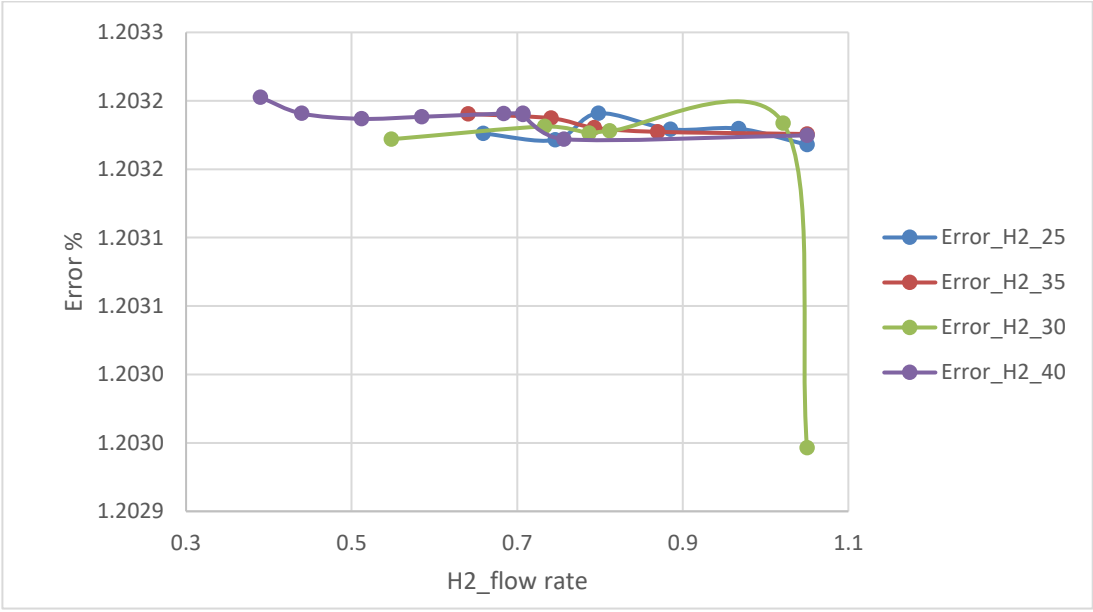

Figure 37 - Error in % between the measured and calculated values of hydrogen production flow rate.

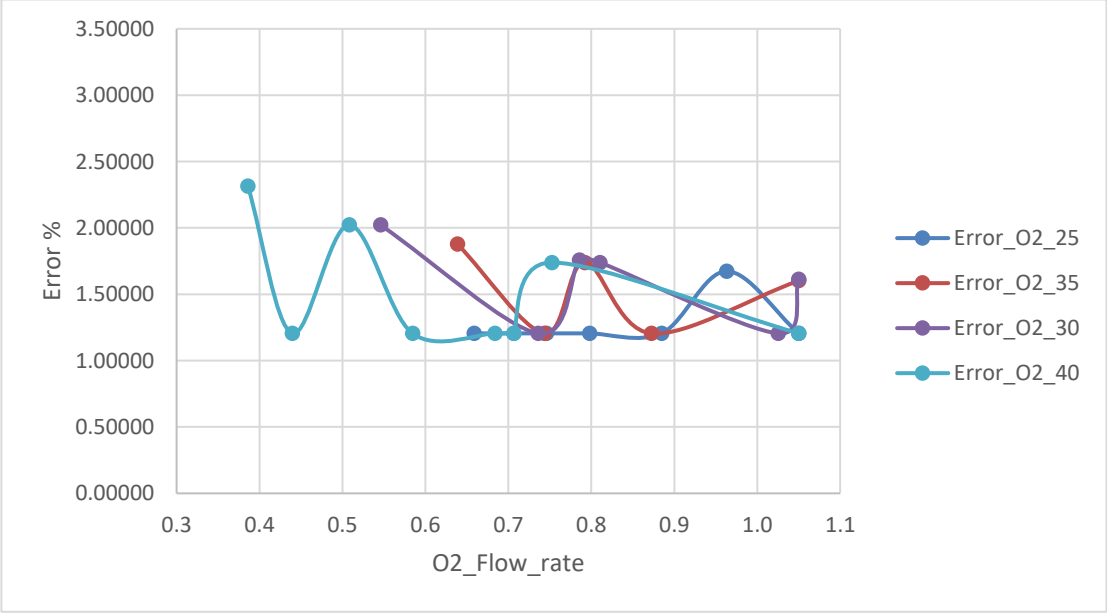

Figure 38 - Error in % between the measured and calculated values of oxygen production flow rate.

The hydrogen and oxygen production flow rates in the Aspen Plus simulation were found to be 1 to 2% higher than the rates observed in experiment. Several factors can account for this discrepancy, which collectively underscore the robustness of our simulation model:

- Aspen Plus operates under idealized conditions that assume perfect system efficiencies and optimal operating parameters. In real-world experiments, various inefficiencies, and minor losses (e.g., energy losses, slight leakages, or suboptimal reaction kinetics) can occur leading to slightly lower production rates.

- The simulation utilizes precise theoretical calculations, while real-world measurements are subject to the precision and accuracy of the instruments used. Small errors in measuring current density, cell voltage, or flow rates can contribute to the observed differences.

- The simulation assumes uniform conditions throughout the electrolyser, such as consistent temperature, pressure, and concentration of the electrolyte. In practice, there can be slight variations in these parameters within the electrolyser cells, affecting the overall efficiency and production rates.

- The Aspen Plus model assumes a pure 18% NaOH electrolyte, whereas the actual electrolyte might contain minor impurities that could impact the electrolysis efficiency slightly.

Despite these minor differences, the close agreement (within 1 to 2%) between the simulated and experimental data indicates that our model is highly accurate and reliable. This small margin of error demonstrates that the Aspen Plus simulation effectively captures the key dynamics of the electrolyser system, providing a valuable tool for predicting performance and optimizing operational conditions.

6.2 Energy efficiency evaluation

In this study, we aim to assess the energy efficiency of an electrolyser system by analyzing the hydrogen production flow rate in relation to the input power.

Previously, we compared the simulated hydrogen flow rates with the experimentally measured values to validate the model. The differences between the simulated and empirical data were then analyzed to quantify the error and understand its sources. This comparison demonstrated that the Aspen Plus simulation results were within 1 to 2% of the real-world measurements, underscoring the model's robustness.

With this validated model, we now turn our focus to assessing the energy

efficiency of the electrolyser system. Energy efficiency will be evaluated by examining the ratio of hydrogen production flow rate to the input power across the different temperature conditions. This analysis will provide insights into the system's performance and identify optimal operating conditions for maximizing energy efficiency in hydrogen production.

Energy efficiency will be assessed as:

$$\eta = \frac{\dot{m_{H2}} * LHV}{P} \qquad (21)$$

where:

η is the energy efficiency of the electrolyzer;

m_{H2} is the mass flow rate of hydrogen produced which must be expressed (kg/s);

Lower Heating Value (LHV) is the lower heating value of hydrogen, which is approximately 120 MJ/kg in standard conditions (temperature 273.15 K and pressure 1 atmosphere);

P is the power input to the electrolyser, measured in watts (W).

The efficiency of an electrolyzer is typically assessed using the LHV of hydrogen. This is because the LHV excludes the energy contained in the water vapour produced during the combustion of hydrogen, making it a more realistic measure of the usable energy content when the hydrogen is used in most practical applications.

HHV (Higher Heating Value) includes the energy of water vapour, assuming it condenses and releases its latent heat. This is less common in practical applications because the water vapour is often not condensed.

Thus, when assessing the efficiency of an electrolyzer, the LHV of hydrogen is generally used. This makes the efficiency values more comparable and relevant to real-world usage scenarios where the full energy of water vapour is not recovered.

Using this formula, the measured and theoretical efficiencies at different temperatures are reported below.

Table 14 - Measured vs Theoretical efficiency at operating temperature of 25°C

Case	T (°C)	Measured Efficiency (%)	Theoretical Efficiency (%)	Error (%)
1.00	25.00	57.59	58.47	1.50
2.00	25.00	59.60	60.51	1.50
3.00	25.00	56.19	57.05	1.50
4.00	25.00	54.79	55.63	1.50
5.00	25.00	55.97	56.83	1.50
6.00	25.00	56.61	57.47	1.50
Avg	**25.00**	**56.79**	**57.66**	**1.50**

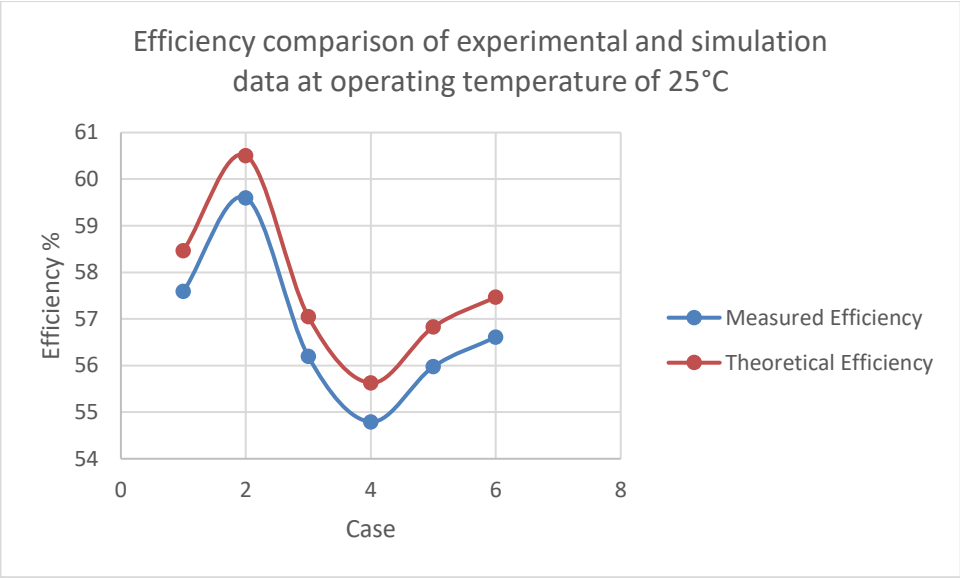

Figure 39 - Efficiency comparison of experimental and simulation data at operating temperature of 25°C

Table 15 - Measured vs Theoretical efficiency at operating temperature of 30°C

Case	T (°C)	Measured Efficiency	Theoretical Efficiency	Error (%)
1.00	30.00	55.47	56.14	1.20
2.00	30.00	59.64	60.36	1.20
3.00	30.00	57.67	58.38	1.20
4.00	30.00	57.03	57.72	1.20
5.00	30.00	55.82	56.50	1.20
6.00	30.00	56.17	56.86	1.20
Avg	**30.00**	**56.97**	**57.66**	**1.20**

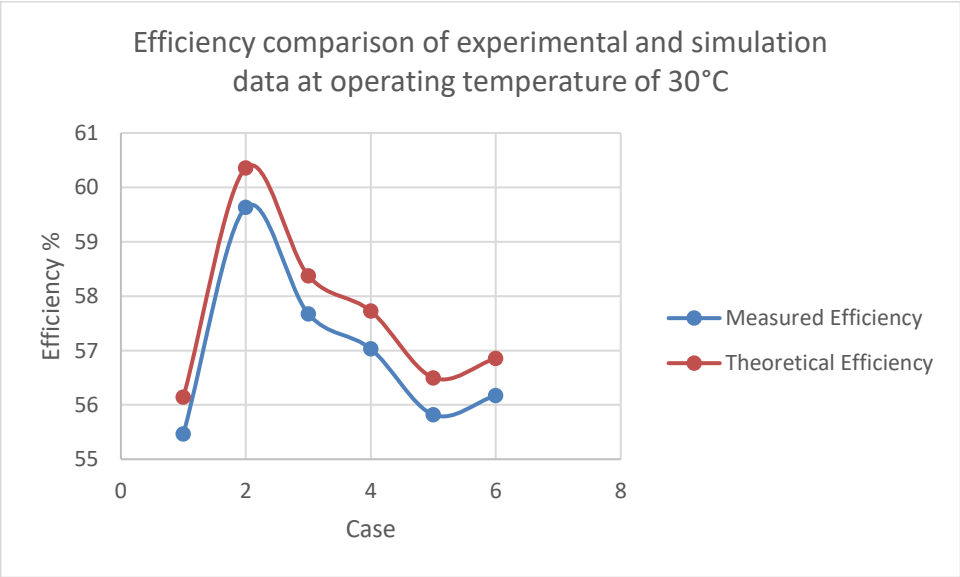

Figure 40 - Efficiency comparison of experimental and simulation data at operating temperature of 30°C

Table 16 - Measured vs Theoretical efficiency at operating temperature of 35°C

Case	T (°C)	Measured Efficiency	Theoretical Efficiency	Error (%)
1	35.00	57.34	58.04	1.20
2	35.00	55.97	56.66	1.20
3	35.00	56.10	56.79	1.20
4	35.00	57.17	57.87	1.20
5	35.00	58.05	58.76	1.20
AVG	**35.00**	**56.93**	**57.62**	**1.20**

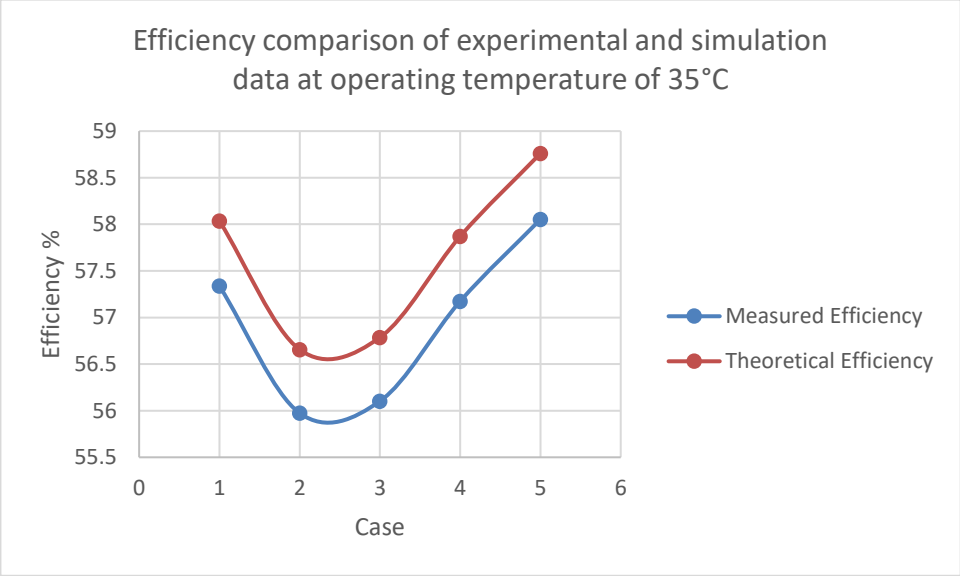

Figure 41 - Efficiency comparison of experimental and simulation data at operating temperature of 35°C

Table 17 - Measured vs Theoretical efficiency at operating temperature of 40°C

Case	T (°C)	Measured Efficiency	Theoretical Efficiency	Error (%)
1	40	58.56	59.27	1.20
2	40	65.87	66.67	1.20
3	40	60.03	60.76	1.20
4	40	59.74	60.46	1.20
5	40	60.55	61.29	1.20
6	40	60.18	60.92	1.20
7	40	62.74	63.51	1.20
8	40	65.09	65.88	1.20
9	40	64.68	65.47	1.20
Avg	**40.00**	**61.94**	**62.69**	**1.20**

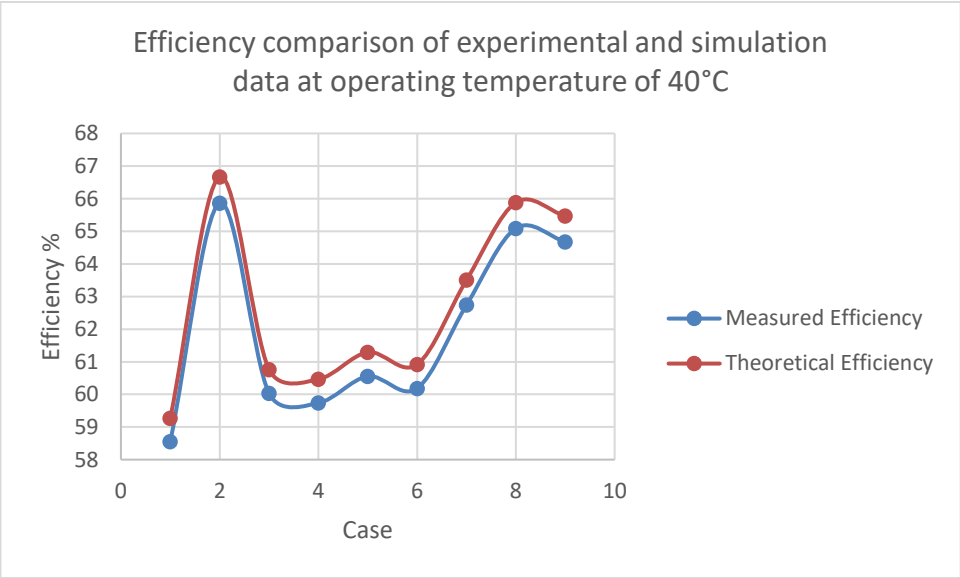

Figure 42 -Efficiency comparison of experimental and simulation data at operating temperature of 40°C

Table 18 - Average measured and theoretical efficiency

T (°C)	Average Measured Efficiency	Average Theoretical Efficiency	Error (%)
25	56.79	57.66	1.50
30	56.97	57.66	1.20
35	56.93	57.62	1.20
40	61.94	62.69	1.20

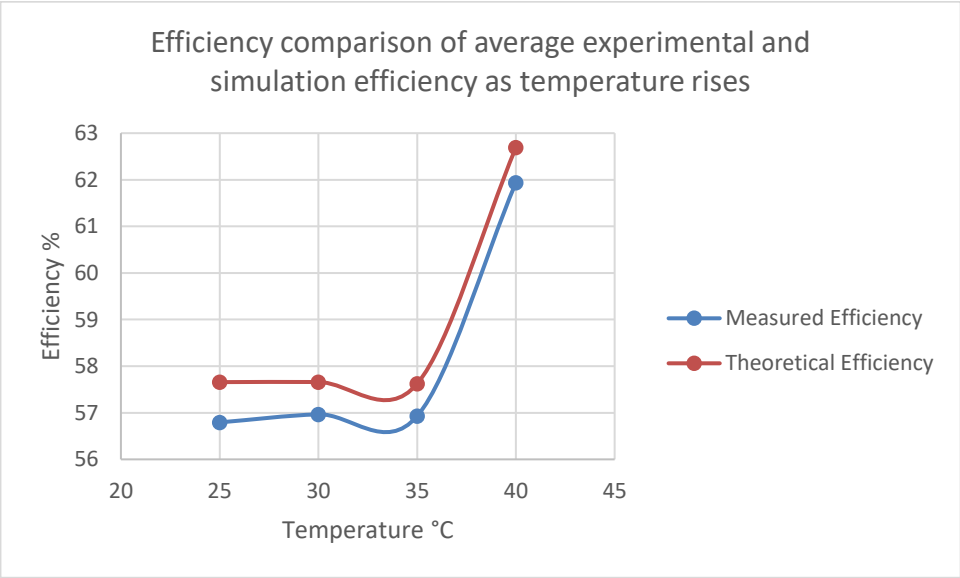

Figure 43 -Efficiency comparison of average experimental and simulation efficiency as temperature rises

Theoretical efficiency calculations are based on conditions that assume no energy losses. In real-world operations, several factors contribute to energy losses, reducing the actual measured efficiency:

- Electrolyzers experience losses due to the resistance of electrical components and connections, causing some input energy to be lost as heat.
- These are additional voltage requirements beyond the thermodynamic minimum needed to drive the electrolysis reaction. They result from kinetic barriers to the reactions occurring at the electrodes.
- Heat generated during the operation can be lost to the surroundings, reducing the overall efficiency.
- Power supplies themselves have inefficiencies, meaning not all the input electrical energy is usable by the electrolyzer.

These practical losses can account for the observed difference of around 1.2% between theoretical and measured efficiencies.

With Rising Temperature, we observe an increase in efficiency because:

- As temperature increases, the activation energy required for the electrolysis reactions decreases. This results in lower overpotentials, meaning less extra voltage is needed to drive the reactions, improving efficiency.

- Higher temperatures improve the ionic conductivity of the electrolyte. Better ionic conductivity means that ions can move more freely through the electrolyte, reducing resistive losses.
- Elevated temperatures increase the reaction rates of the electrochemical processes. This means that the electrolyzer can operate more effectively, requiring less energy to achieve the same level of hydrogen production.
- At higher temperatures, the solubility of gases in the electrolyte decreases, leading to less gas bubble formation on the electrodes. Gas bubbles can act as barriers to ion flow, so reducing their formation improves efficiency.

In summary, while theoretical efficiency offers a benchmark, measured efficiency accounts for practical operational challenges.

CONCLUSIONS

This study successfully used Aspen Plus to develop a detailed model of an AWE system, encompassing electrochemical behaviour and interactions between system components. The model's flexibility and ability to integrate enabled accurate predictions of system performance under various temperature conditions.

The AWE system model, consisting of an electrolysis stack, heater, pumps, and phase separators, effectively simulates the production and purification of hydrogen and oxygen gases.

The use of RStoic reactor blocks for modelling electrochemical reactions allowed for a simplified yet accurate representation of the core processes within the electrolysis stack.

The electrolyzer stack, modelled with RStoic reactors and separator blocks, demonstrated efficient separation of hydrogen and oxygen gases from the liquid electrolyte.

The simulation was tuned using empirical data from experiments conducted at various temperatures, ensuring that the model accurately reflected real-world operational characteristics.

The simulation results for hydrogen and oxygen flow rates were within 1-2% of the empirically measured data, validating the accuracy of the Aspen Plus model.

Aspen Plus simulations assume perfect system efficiencies without accounting

for real-world losses such as energy dissipation, minor leakages, and suboptimal reaction kinetics. These idealized conditions contribute to the slight overestimation of hydrogen and oxygen production rates. Real-world measurements are influenced by the precision and accuracy of the instruments used. Even small errors in measuring current density, cell voltage, or flow rates can lead to discrepancies between simulated and empirical data.

The experiments were conducted at various temperatures (25°C, 30°C, 35°C, 40°C) and a constant pressure of 4.5 bar. The results show that both the simulated and measured hydrogen and oxygen production rates increase with temperature, reflecting the enhanced electrochemical activity at higher temperatures. The consistent pressure helps isolate the temperature effects, making the analysis more straightforward.

The study underscores the robustness of Aspen Plus as a tool for modelling and optimizing hydrogen production systems. Future work can focus on refining the model to account for real-world inefficiencies and integrating more detailed kinetic data to further enhance its predictive capabilities.

LIST OF FIGURES

LIST OF TABLES

REFERENCES

[1] https://www.iea.org/data-and-statistics/data-tools/greenhouse-gas-emissions-from-energy-data-explorer

[2] https://www.iea.org/data-and-statistics/data-tools/energy-statistics-data-browser?country=WORLD&fuel=Energy%20supply&indicator=TESbySource

[3] https://www.iea.org/data-and-statistics/data-tools/energy-statistics-data-browser?country=WORLD&fuel=Energy%20consumption&indicator=TFCShareBySector

[4] Framework Convention on Climate Change, Copenhagen Accord (Point 3) https://unfccc.int/resource/docs/2009/cop15/eng/l07.pdf

[5] Renewable Energy Sources and Climate Change Mitigation; Renewable Energy in the Context of Sustainable Development - Chapter 9, page 731

[6] Renewable Energy Sources and Climate Change Mitigation; Renewable Energy in the Context of Sustainable Development - Chapter 9, page 728

[7] European Green Deal https://eur-lex.europa.eu/resource.html?uri=cellar:b828d165-1c22-11ea-8c1f-01aa75ed71a1.0002.02/DOC_1&format=PDF

[8] Italy 2023 Energy Policy Review – International Energy Agency

[9] Clean Hydrogen Monitor, November 2023 https://hydrogeneurope.eu/wp-content/uploads/2023/10/Clean_Hydrogen_Monitor_11-2023_DIGITAL.pdf

[10] https://www.h2inframap.eu/

[11] A review on recent trends, challenges, and innovations in alkaline water electrolysis, Abdelrahman S. Emam, Mohammad O. Hamdan , Bassam A. Abu-Nabah, Emad Elnajjar https://doi.org/10.1016/j.ijhydene.2024.03.238

[12] Hydrogen production by PEM water electrolysis – A review S. Shiva Kumar, V. Himabindu Centre for Alternative Energy Options, Institute of Science and Technology, Jawaharlal Nehru Technological University Hyderabad, Kukatpally, Hyderabad, Telangana 500085, India

[13] Hydrogen production by PEM water electrolysis – A review S. Shiva Kumar, V. Himabindu https://sci-hub.se/downloads/2019-10-21/c7/shivakumar2019.pdf

[14] Advancements, strategies, and prospects of solid oxide electrolysis cells (SOECs): Towards enhanced performance and large-scale sustainable hydrogen production, Amina Lahrichi, Youness El Issmaeli, Shankara S. Kalanur, Bruno G. PolleT https://doi.org/10.1016/j.jechem.2024.03.020

[15] Design of an Alkaline Electrolysis Stack, Yakdehige Sanath Kumara De Silvi https://core.ac.uk/download/pdf/225893186.pdf

[16] Influence of operation parameters in the modeling of alkaline water electrolyzers for hydrogen production, Ernesto Amores, Jesús Rodríguez, Christian Carreras https://doi.org/10.1016/j.ijhydene.2014.07.001

[17] A Comprehensive Survey of Alkaline Electrolyzer Modeling: Electrical Domain and Specific Electrolyte Conductivity by Frank Gambou,Damien Guilbert, Michel Zasadzinski and Hugues Rafaralahy https://www.mdpi.com/1996-1073/15/9/3452#B39-energies-15-03452

[18] https://www.erreduegas.it/wp-content/uploads/brochure_mercury_2019.pdf

[19] Low-temperature electrolysis system modelling: A review by Pierre Olivier, Cyril Bourasseau, Pr. Belkacem Bouamama https://doi.org/10.1016/j.rser.2017.03.099